(4)

TECHNICAL REPORT BRL-TR-3077

BRL

ONE-DIMENSIONAL ANALYSIS OF A LIQUID JET IN A REGENERATIVE LIQUID PROPELLANT GUN

GLORIA P. WREN
PAUL S. GOUGH

APRIL 1990

U.S. ARMY LABORATORY COMMAND

BALLISTIC RESEARCH LABORATORY
ABERDEEN PROVING GROUND, MARYLAND

NOTICES

Destroy this report when it is no longer needed. DO NOT return it to the originator.

Additional copies of this report may be obtained from the National Technical Information Service, U.S. Department of Commerce, 5285 Port Royal Road, Springfield, VA 22161.

The findings of this report are not to be construed as an official Department of the Army position, unless so designated by other authorized documents.

The use of trade names or manufacturers' names in this report does not constitute indorsement of any commercial product.

REPORT DOCUMENTATION PAGE

Form Approved
OMB No. 0704-0188

1. AGENCY USE ONLY (Leave blank)	2. REPORT DATE	3. REPORT TYPE AND DATES COVERED
	April 1990	Final, Jan 89 - Jan 90

4. TITLE AND SUBTITLE
One-Dimensional Analysis of a Liquid Jet in a Regenerative Liquid Propellant Gun

5. FUNDING NUMBERS
C: DA306709444600

6. AUTHOR(S)
Wren, Gloria P. and *Gough, Paul S.

7. PERFORMING ORGANIZATION NAME(S) AND ADDRESS(ES)

8. PERFORMING ORGANIZATION REPORT NUMBER

9. SPONSORING / MONITORING AGENCY NAME(S) AND ADDRESS(ES)
US Army Ballistic Research Laboratory
ATTN: SLCBR-DD-T
Aberdeen Proving Ground, MD 21005-5066

10. SPONSORING / MONITORING AGENCY REPORT NUMBER
BRL-TR-3077

11. SUPPLEMENTARY NOTES
Paul Gough Associates, 1048 South Street, Portsmouth, NH 03801-5423

12a. DISTRIBUTION / AVAILABILITY STATEMENT
Approved for public release; distribution unlimited

12b. DISTRIBUTION CODE

13. ABSTRACT *(Maximum 200 words)*

In the regenerative liquid propellant gun (RLPG) a liquid monopropellant is injected by a moving piston in the form of an annular jet from a reservoir into a combustion chamber. Currently there are a number of lumped parameter models of the RLPG in use in the United States. However, the structure and spatial extension of the jet are not considered in any of these models. In this report the details of the jet description in the first fully one-dimensional continuum model of the RLPG in the United States is presented. Jet structure and ballistic performance in terms of pressures, pressure gradients, muzzle velocity and accumulation are examined for varying jet breakup conditions. The major conclusions are: (1) jet breakup length has a modest impact on ballistic performance in terms of muzzle velocity and maximum chamber pressure for the 25-mm gun considered compared to ballistic performance predicted by a lumped parameter simulation, and (2) the one-dimensional representation of a jet produces a pressure gradient which is significantly different from the pressure gradient currently used in lumped parameter simulations.

14. SUBJECT TERMS	15. NUMBER OF PAGES
Regenerative Liquid Propellant Gun; Taylor Theory; One-Dimensional Model; Jet Breakup Length	68
	16. PRICE CODE

17. SECURITY CLASSIFICATION OF REPORT	18. SECURITY CLASSIFICATION OF THIS PAGE	19. SECURITY CLASSIFICATION OF ABSTRACT	20. LIMITATION OF ABSTRACT
UNCLASSIFIED	UNCLASSIFIED	UNCLASSIFIED	SAR

GENERAL INSTRUCTIONS FOR COMPLETING SF 298

The Report Documentation Page (RDP) is used in announcing and cataloging reports. It is important that this information be consistent with the rest of the report, particularly the cover and title page. Instructions for filling in each block of the form follow. It is important to ***stay within the lines*** to meet ***optical scanning requirements***.

Block 1. Agency Use Only *(Leave blank)*.

Block 2. Report Date. Full publication date including day, month, and year, if available (e.g. 1 Jan 88). Must cite at least the year.

Block 3. Type of Report and Dates Covered. State whether report is interim, final, etc. If applicable, enter inclusive report dates (e.g. 10 Jun 87 - 30 Jun 88).

Block 4. Title and Subtitle. A title is taken from the part of the report that provides the most meaningful and complete information. When a report is prepared in more than one volume, repeat the primary title, add volume number, and include subtitle for the specific volume. On classified documents enter the title classification in parentheses.

Block 5. Funding Numbers. To include contract and grant numbers; may include program element number(s), project number(s), task number(s), and work unit number(s). Use the following labels:

C	- Contract	PR	- Project
G	- Grant	TA	- Task
PE	- Program Element	WU	- Work Unit Accession No.

Block 6. Author(s). Name(s) of person(s) responsible for writing the report, performing the research, or credited with the content of the report. If editor or compiler, this should follow the name(s).

Block 7. Performing Organization Name(s) and Address(es). Self-explanatory.

Block 8. Performing Organization Report Number. Enter the unique alphanumeric report number(s) assigned by the organization performing the report.

Block 9. Sponsoring/Monitoring Agency Name(s) and Address(es). Self-explanatory.

Block 10. Sponsoring/Monitoring Agency Report Number. *(If known)*

Block 11. Supplementary Notes. Enter information not included elsewhere such as: Prepared in cooperation with...; Trans. of...; To be published in.... When a report is revised, include a statement whether the new report supersedes or supplements the older report.

Block 12a. Distribution/Availability Statement. Denotes public availability or limitations. Cite any availability to the public. Enter additional limitations or special markings in all capitals (e.g. NOFORN, REL, ITAR).

DOD	- See DoDD 5230.24, "Distribution Statements on Technical Documents."
DOE	- See authorities.
NASA	- See Handbook NHB 2200.2.
NTIS	- Leave blank.

Block 12b. Distribution Code.

DOD	- Leave blank.
DOE	- Enter DOE distribution categories from the Standard Distribution for Unclassified Scientific and Technical Reports.
NASA	- Leave blank.
NTIS	- Leave blank.

Block 13. Abstract. Include a brief *(Maximum 200 words)* factual summary of the most significant information contained in the report.

Block 14. Subject Terms. Keywords or phrases identifying major subjects in the report.

Block 15. Number of Pages. Enter the total number of pages.

Block 16. Price Code. Enter appropriate price code *(NTIS only)*.

Blocks 17. - 19. Security Classifications. Self-explanatory. Enter U.S. Security Classification in accordance with U.S. Security Regulations (i.e., UNCLASSIFIED). If form contains classified information, stamp classification on the top and bottom of the page.

Block 20. Limitation of Abstract. This block must be completed to assign a limitation to the abstract. Enter either UL (unlimited) or SAR (same as report). An entry in this block is necessary if the abstract is to be limited. If blank, the abstract is assumed to be unlimited.

TABLE OF CONTENTS

INTENTIONALLY LEFT BLANK.

LIST OF FIGURES

1. INTRODUCTION

In the Regenerative Liquid Propellant Gun (RLPG) a liquid monopropellant is injected by a moving piston from a reservoir into the combustion chamber. The resulting combustion gases not only create a pressure differential between the combustion chamber and liquid reservoir which perpetuates the injection of the fluid, but, together with unburned propellant, flow into the gun tube and accelerate the projectile. A number of gun design concepts have been proposed to deliver the liquid monopropellant to the combustion chamber. The design used as the basis of this report is shown in Figure 1. In this concept the center bolt is stationary, and the outer piston moves rearward to inject the propellant as an annular sheet into the combustion chamber.

Currently there are a number of lumped parameter models of the RLPG in use in the United States.[1-3] These differ in modeling the details of the delay in energy release due to the finite time of breakup and combustion of the liquid propellant. However, the structure and spatial extension of the jet are not considered in any of the models. Moreover, the momentum of the entering liquid propellant is assumed to be entirely dissipated in the combustion chamber, the contents of which are presumed to be in a condition of stagnation relative to the gun. As a result, artificially large pressure drops may be predicted for the gas flowing from the combustion chamber into the tube for some configurations. From a practical systems point of view this may result in overestimation of pressures, resulting in inaccurate estimates of required gun tube wall thickness and gun mass.

The assumption of stagnation in the combustion chamber may have been appropriate to early RLPG designs which involved a large number of small jets. However, current designs make use of a single annular jet which may well enter the gun tube prior to complete disintegration. Accordingly, the momentum of the jet may not be dissipated in the combustion chamber, and the pressure drop between the combustion chamber and the gun tube may be considerably less than is predicted by current models in the case that the jet extends into the tube. Apart from a theoretical interest in the jet breakup length as a modeling detail, intuition suggests that there may be a significant ballistic consequence in the sense that a greater breakup length may permit the attainment of a given muzzle velocity at a lower maximum chamber pressure due to the flow of propellant in the tube. However, this study shows that gun performance is not significantly enhanced with an extended liquid jet.

In this report the details of the first fully one-dimensional continuum model of the RLPG[4] in the United States are presented in which a liquid jet is represented explicitly. Jet structure and

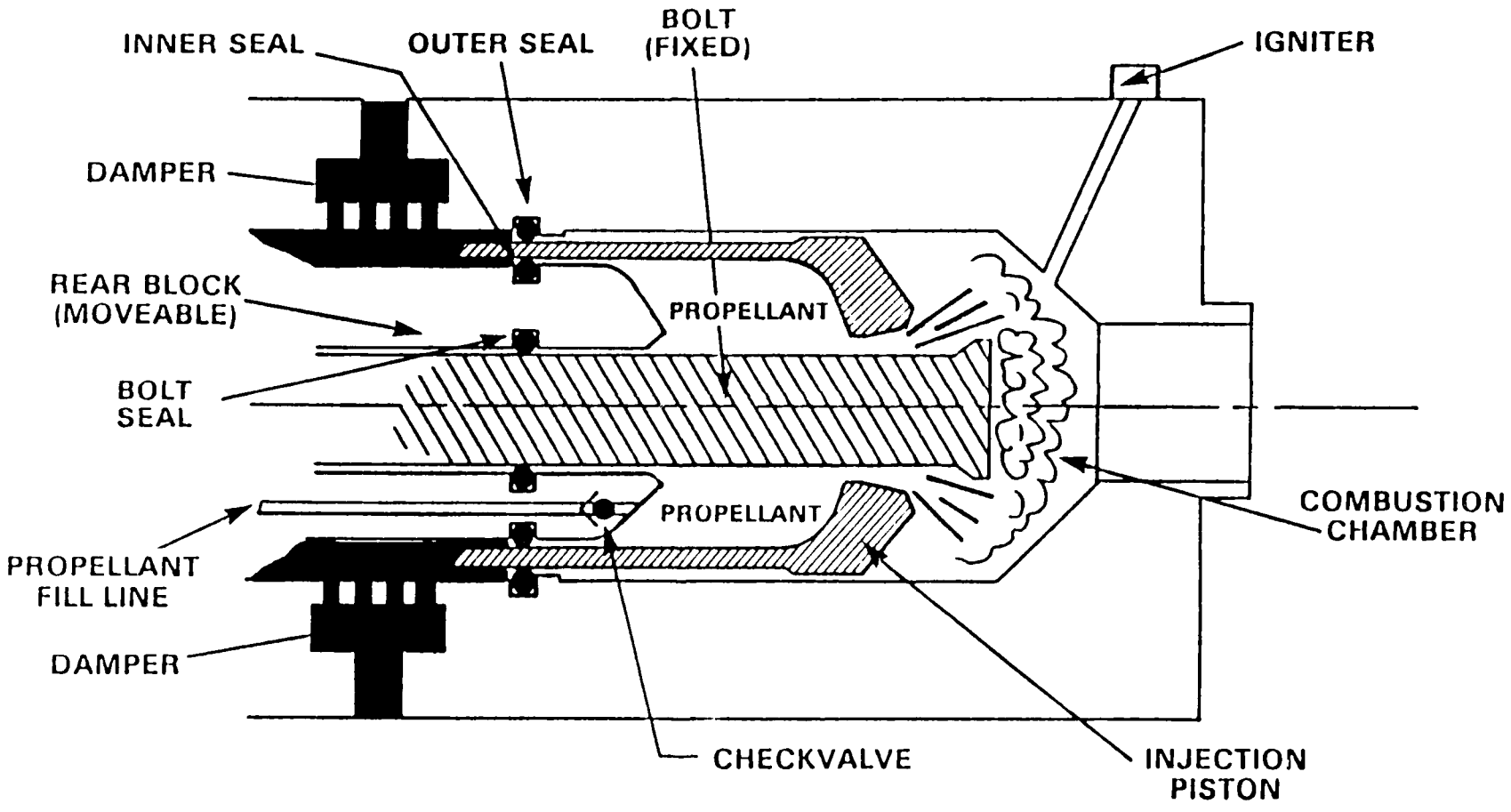

Figure 1. Regenerative Liquid Propellant Gun with a Stationary Center Bolt.

ballistic performance in terms of pressures, pressure gradients and muzzle velocity are examined for varying jet breakup conditions. Finally, current areas of investigation such as liquid propellant accumulation in the combustion chamber are related to the jet description.

2. 1-D MODEL OF JET IN RLPG

The combustion process of the injected liquid propellant in the RLPG is most simply represented in lumped parameter models as instantaneous combustion. The injected propellant is assumed to atomize so finely and so completely upon injection into the combustion chamber that the chemical energy is released within a ballistically negligible time interval. Experimental evidence, however, indicates that for designs of present interest the time delay required to release the chemical energy is not negligible relative to the overall ballistic time scale.[5-7] Accordingly, lumped parameter codes have often included options to break up the injected propellant into droplets of a user defined size which burn at a finite rate. In general, no consideration is given to the hydrodynamic delay associated with the decomposition of the injected jet into droplets. Experimental data, however, has indicated that a substantial fraction of the total propellant liquid propellant charge may accumulate in unreacted form in the combustion chamber, and the resulting accumulation can significantly affect the overall ballistic behavior.[5-7]

Thus, incorporation of a hydrodynamic delay due to the finite rate of jet breakup is considered to be necessary to improve simulations of RLPG behavior. Although delayed energy release may be addressed within a lumped parameter representation, the coupling of the jet breakup length to the axial geometry of the combustion chamber requires a one-dimensional formulation. It is of interest to examine the possibility that the jet intrudes into the tube and even impacts the base of the projectile. Since the tube may have a significantly smaller diameter than the combustion chamber, the release of a given amount of energy in the tube would result in a greater local rate of pressurization than it would in the chamber. Energy release in the tube could have a marked effect on the relationship between the chamber pressure and the tube pressure.

Lumped parameter representations have also assumed a state of stagnation in the combustion chamber. The stagnation assumption is appropriate if the jet is completely disintegrated within the combustion chamber and if the cross-sectional area of the chamber is much larger than that of the tube. Some simulations have revealed a large pressure drop between the chamber and the tube as the stagnant gas in the chamber is accelerated to near sonic conditions at the entrance to the tube, following sufficient motion of the projectile. A quite different result would occur if the jet is

represented as retaining a coherent structure throughout the chamber and into the tube, with implications for both gun performance and estimate of required gun tube thickness. In addition, a continuum analysis permits the retention of the momentum of the jet and of the droplets into which it disintegrates.

The representation of the distributed jet within a one-dimensional continuum formulation is shown in Figure 2 for a configuration in which both the inner and outer pistons move rearward. However, the one-dimensional model is pertinent to all regenerative geometries of current and past interest including Concepts VI, VIA, VIB, VIC, RAP, Traveling Charge and the "shower-head" which vary in the details of the piston movement and liquid injection. Other configurations may be represented as well. The governing equations for the combustion chamber are the same as those of the tube. When droplets are present, the governing equations consist of one-dimensional balances of mass, momentum and energy for the mixture of combustion gases and droplets. Slip between the gas and droplets is not considered, and the mixture is said to be in mechanical equilibrium. The cross-sectional area of flow in each of the regions of the combustion chamber or tube is that of the chamber or tube reduced by the cross-sectional area of the jet. The flow area may also be reduced due to the intrusion of the center bolt.

The representation depicted in Figure 2 permits the jet to be partially reflected from the chamber face and partially transmitted into the tube, and to be reflected from the projectile base. The reflected portions of the jet may return to the piston face and reflect again, if their disintegration is sufficiently slow. The jet increments follow an inertial path and do not interact with one another. Thus, the jet area, mass addition and momentum addition at any location may consist of an aggregate of jet increments. The resulting distribution of jet properties may be highly structured and non-uniform. To avoid the risk of numerical instability, the source terms are smoothed using a simple numerical filter. However, the state variables of density, pressure, velocity and porosity for the mixture result directly from the response of the finite difference equations to the smoothed source terms.

The two major physical modeling assumptions requiring comment are the fixed rate of decomposition of the jet and the inertial trajectories of the jet increments. At present there is insufficient experimental data to adequately characterize the rate of breakup and disintegration of the liquid jet. The lack of direct experimental data is due in part to the high pressures in the gun and the difficulty in penetrating combustion products. Thus, the representation of the distributed jet adopted in this report is intended to allow the study of the influence of the jet on ballistic

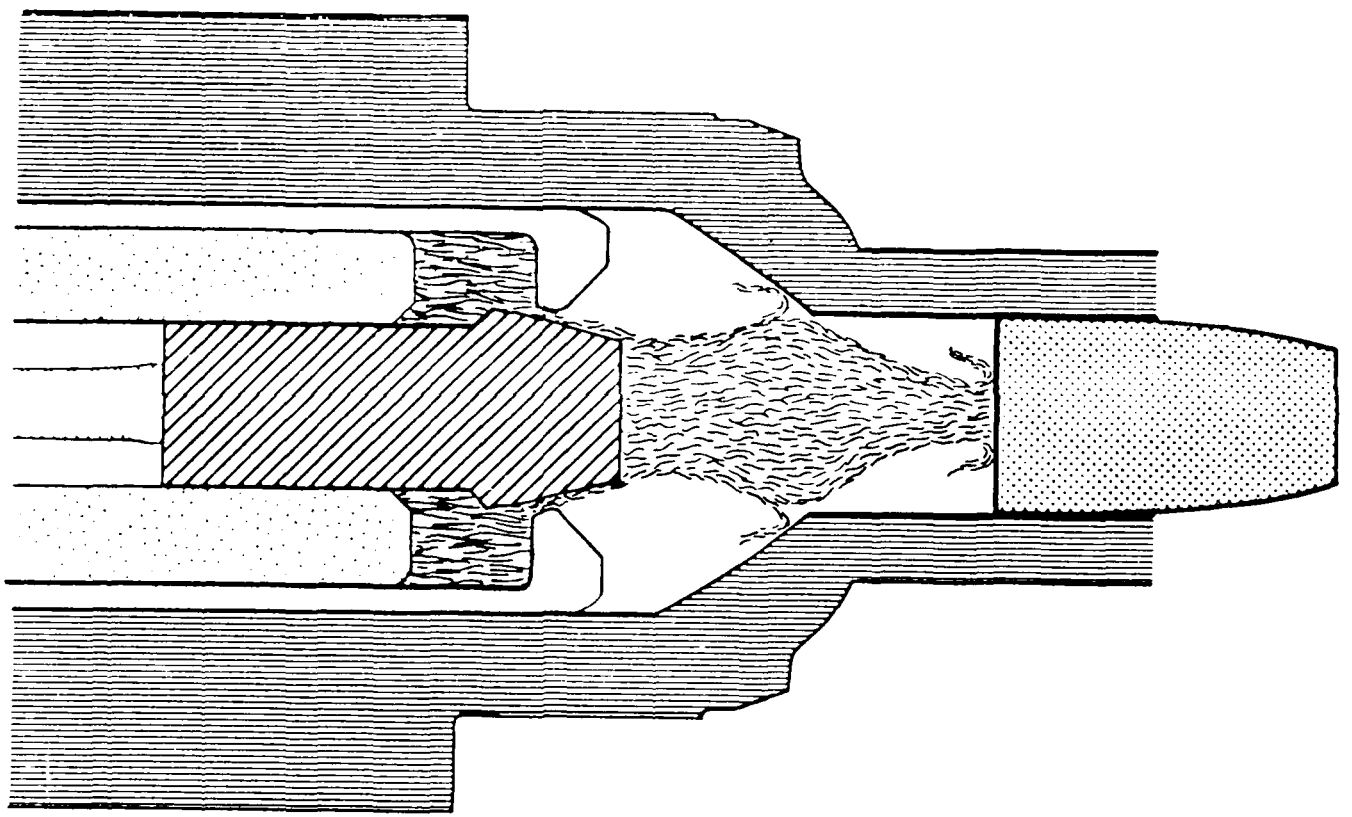

Figure 2. Jet Representation with Possible Reflection in Liquid Propellant Gun with Two Moving Pistons.

performance. A predictive function is not intended and is, in fact, precluded by a lack of constitutive data.

In addition, the assumption that each jet increment follows a purely inertial path is felt to be a reasonable first approximation provided that the fraction of the available cross-sectional area occupied by the jet is not too large. The jet is radially unconfined from a continuum perspective. Since the jet is much less compressible than the surrounding mixture, it is expected that the axial pressure distribution within the jet is controlled by the dynamics of the mixture. As one portion of the jet presses against another, the radial boundary of the jet is expected to displace to accommodate the interaction. Only when the jet begins to fill the cross-sectional area does this assumption break down requiring the consideration of an axial stress field in the jet independent of that in the mixture. Considering other forces acting on the jet, the gas-dynamic forces are drag and buoyancy. Drag forces are expected to exert a negligible influence on the momentum of the jet; the associated shear is accommodated by the liquid converted to droplets. The buoyancy force is simply due to gradients of the gas pressure. Although the gas pressure gradient can become large, especially at the entrance to the tube, the density of the jet is much greater than that of the gas, and the neglect of its influence on the jet is felt to be justified as a first approximation.

The finite rate of decomposition is applied to a jet increment introduced into the combustion chamber as a result of the boundary values of liquid and chamber pressure on each side of the piston face. The properties of the liquid discharge are averaged over a sample time interval and at the conclusion of the interval an elementary jet increment is defined. The increment is characterized by initial values of its mass, velocity and location as well as the time at which it is formed. In addition, it is assumed that its rate of decomposition is fixed by the conditions which prevail, on average, during the sampling interval.

The breakup of the jet is governed by Taylor's theory.[8] Taylor's theory is an aerodynamic theory for a circular jet which treats the primary atomization of the jet. The theory may be most applicable to the early ignition phase of the RLPG, and its applicability to the later high pressure phase is questionable since other mechanisms such as those considered in turbulent theory may apply.[8] The theory provides a jet breakup length which is dependent on local flow conditions and which assumes asymptotic behavior in two limiting cases depending on the value of a parameter B. Since the theory provides no guidance between the two limiting cases, the jet breakup length is determined by linear interpolation for values of B between the two limiting cases. The parameter B is the ratio of the Reynold's number to the Weber number, that is

$$B = \frac{Re}{We} = \frac{2\rho VD/\mu}{2\rho V^2 D/\sigma} = \frac{\sigma}{\mu V}$$

with μ the viscosity, σ the surface tension, ρ the density, V the velocity, and D the diameter. In the case of an annulus, the diameter, D, is taken to be the hydraulic diameter, that is, twice the gap. The Reynolds number compares the momentum force to the viscous force. Larger values indicate an increased likelihood of turbulence. The Weber number compares a momentum force to a surface tension force. Larger Weber numbers indicate an increased likelihood of breakup. Thus, the parameter B compares forces attempting to hold the jet together with those attempting to pull it apart. Estimates[9] of the Reynolds number and Weber number for the RLPG are high, that is, $>10^4$. It is noted that the Taylor theory, and, in fact, most theories of jet breakup, apply to cylindrical orifices rather than the annular orifice of the RLPG. In addition, the regime of pressure in which the RLPG operates may be supercritical for at least a part of the pressurization cycle[10] suggesting to some researchers[11] that the spray should behave like a turbulent jet since capillary forces due to surface tension would no longer play a role. Thus, the Taylor theory utilized in this model is not expected to be predictive. However, it does allow the study of ballistic effects of extended jets in the RLPG.

The constitutive law governing the rate of breakup of the liquid jet gives a jet breakup length, x_B, determined from the following function.

For

$$\frac{\rho_L}{\rho_G} B^2 > 10$$

where ρ_L is the liquid density, ρ_G is the gas density, and B is the ratio of the Reynold's number to the Weber number, the corresponding jet breakup length is

$$X_B = (JBUC)D \left(\frac{\rho_L}{\rho_G}\right)^{\frac{1}{2}}$$

where D is the diameter of the jet, and JBUC is the jet breakup coefficient supplied by the user.

For

$$0.1 \leq \frac{\rho_L}{\rho_G} B^2 \leq 10$$

the corresponding jet breakup length is

$$X_B = (JBUC)D \left(\frac{\rho_L}{\rho_G}\right)^{\frac{1}{2}} \left[\frac{\frac{\rho_L}{\rho_G}B^2 - .1}{9.9}\right] + (JBUC)D \left(\frac{\rho_L}{\rho_G B}\right)^{\frac{1}{3}} \left[\frac{\frac{\rho_L}{\rho_G}B^2 - 10}{-9.9}\right].$$

For

$$\frac{\rho_L}{\rho_G}B^2 < 0.1$$

the corresponding jet breakup length is

$$X_B = (JBUC)D \left(\frac{\rho_L}{\rho_G B}\right)^{\frac{1}{3}}.$$

In this study, the following options are selected for the jet representation. The jet is fully admitted into the tube, and the droplets formed by disintegration of the jet are instantaneously combusted. A value is supplied for JBUC, the jet breakup coefficient in the Taylor theory. In general for a given geometry, as JBUC increases the jet breakup length increases and the jet disintegrates more slowly. The value of JBUC may be increased until the tube becomes filled with liquid, terminating gas flow in the tube. The Taylor formulation is also responsive to the thickness of the jet, with thicker jets corresponding to a larger jet breakup length for a given geometry and user supplied value of JBUC.

3. MESH INDIFFERENCE

The data set chosen for this study is that of a 25-mm regenerative liquid propellant test fixture with a projectile mass of 97.3 grams with gun and propellant parameters shown in Appendix A. The mesh indifference of the solution was assessed by the performance factors of maximum chamber and liquid pressures as well as muzzle velocity for the 25-mm gun. The jet breakup coefficient (JBUC) chosen for the mesh indifference study was 0.5, a value which results in a distinct jet extending into the chamber and at times into the tube. The results appear in the table below. As can be seen from the table, the range of maximum chamber and liquid pressures is on the order of 2.9% and 1.8% from highest to lowest, respectively, while the range in muzzle velocity is about 0.5%.

The numerical solution algorithm uses local conditions of mass and energy balance, and does not enforce global conservation apriori. Accordingly, the degree to which these differ is a check on the accuracy of the equations. The differences are reported throughout the calculation. It is the

Table 1. Mesh Indifference of Nominal Data Base.

Number of Mesh Points Tube, Chamber	Maximum Chamb Pressure (MPa)	Maximum Liquid Pressure (MPa)	Muzzle Velocity (m/s)	Max Final Mass Defect (%)	Max Final Energy Defect (%)
				0.864	
41, 21	336.72	345.32	1486.0	1.278	1.344
41, 11	326.71	349.51	1487.1	1.172	1.756
51, 11	328.37	350.69	1479.2	1.097	1.718
61, 11	331.08	351.82	1479.2		1.734

maximum difference between the total initial mass and the mass at any timestep which is reported as the maximum final mass defect. Similarly, the maximum difference between the total initial energy and the energy at any timestep is reported as the maximum final energy defect. The mass and energy defects are in the 1.5% range for most mesh spacings. Thus, since the results are similar for all mesh sizes considered, values of 41 mesh points in the tube and 21 points in the liquid and combustion chambers were chosen for the study due to the lower mass and energy error

4. JET STRUCTURE

As shown in Figure 2, the jet can extend through the combustion chamber and into the tube. As the jet breakup coefficient (JBUC) is increased from 0.2 to 0.9 for the given geometry, the jet disintegrates more slowly and extends further through the combustion chamber, eventually entering the tube. Figure 3 illustrates the evolution of the jet for a JBUC of 0.9, the jet containing the most mass for the 25-mm gun which did not fill the tube with liquid. The forward axis represents axial location where 0.0 is the initial piston position and 1.39 cm is the entrance to the tube. The vertical axis represents the mass per unit length of the jet. The mass per unit length is chosen for the representation since the actual size of the numeric spacing varies as the piston moves rearward. Finally, the horizontal axis displays the time and provides a view of the jet evolution at 1.0 ms, 1.5 ms, 2.0 ms, 2.5 ms, 3.0 ms and 3.5 ms.

At 1.0 ms a portion of the propellant which has been injected is in the chamber in the form of unburned liquid. As the piston moves rearward, a segment of the jet can be seen at the piston face. Unburned liquid propellant extends forward through the combustion chamber and into the tube. In the case of the large JBUC of 0.9 represented in Figure 3, a significant amount of mass

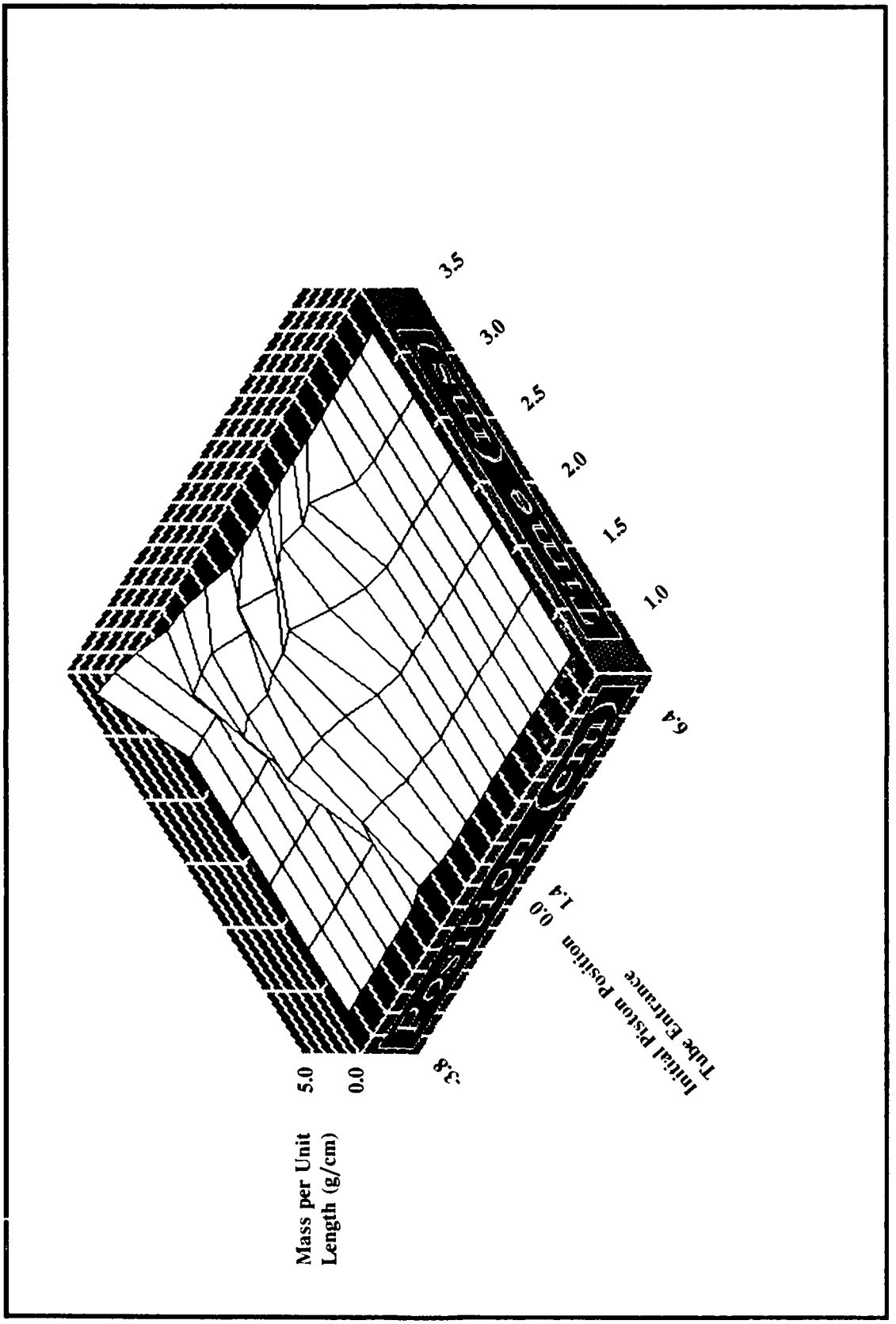

Figure 3. Evolution of jet with JBUC=0.9.

accumulates in the jet, and the jet is structured and irregular at times. It is noted that the jet breakup length may vary for each injected mass of propellant, and, thus, the jet consists of mass which is disintegrating slowly as well as mass which is releasing energy more readily.

The value of the parameter $B = \frac{\sigma}{\mu V}$ is inversely proportional to the jet velocity since the surface tension and the viscosity of the liquid are taken to be constant. During the startup regime the jet velocity at the entrance to the combustion chamber is unsteady and varies from 0.0 to approximately 3500 cm/sec. The value of the Taylor parameter, $\frac{\rho_L}{\rho_G} B^2$, for a JBUC of 0.9, reflects the variation in liquid velocity over the first millisecond and first increases and then decreases with values between 2 and 10. Between 1.0 and 2.0 milliseconds the value of the Taylor parameter drops as the jet velocity increases from 2 to approximately 0.1, the transition value for the jet breakup length constitutive law. The vent does not fully open until approximately 2.0 milliseconds. For the remainder of the ballistic cycle the value of the Taylor parameter is less than 0.1, reflecting the high jet velocity of up to 20000 cm/sec. End of injection occurs at about 3.7 ms with projectile exit at 4.8 ms.

The distribution of mass between liquid propellant in the liquid reservoir booster, the gas in the combustion chamber and tube, and the jet is shown in Figures 4 and 5 for JBUCs of 0.6 and 0.9, respectively. The distribution of mass is displayed at each ms between 0.0 ms and projectile exit at about 4.6 ms for JBUC=0.6 and projectile exit at 4.83 ms for JBUC=0.9. The liquid mass in the droplets which are stripped from the jet is instantaneously combusted in this simulation. As expected, the larger jet breakup coefficient of 0.9 is associated with greater accumulation of unburned liquid propellant in the combustion chamber and tube than the JBUC of 0.6. Figure 4 for JBUC=0.6 shows up to 10% of mass in the jet during the ballistic event, and Figure 5 for JBUC=0.9 shows up to 20% of the mass in the jet. Thus, a significant amount of mass can accumulate in the combustion chamber in the form of liquid in the jet. If the jet is represented with droplets stripped from the jet which burn according to a pressure-dependent burn rate, then additional accumulation could occur. In general, as the jet breakup coefficient increases, more mass accumulates in the jet.

In order to provide a framework for the discussion which follows, it is helpful to categorize the various jet breakup coefficients into three general categories for the 25-mm gun considered here. "Small" JBUCs will be used to refer to coefficients of 0.1 to 0.4 in which the jet is confined to the combustion chamber. "Moderate" JBUCs will be used to refer to coefficients of 0.5 to 0.7 in which the jet stays primarily within the combustion chamber, but intrudes into the tube for a short

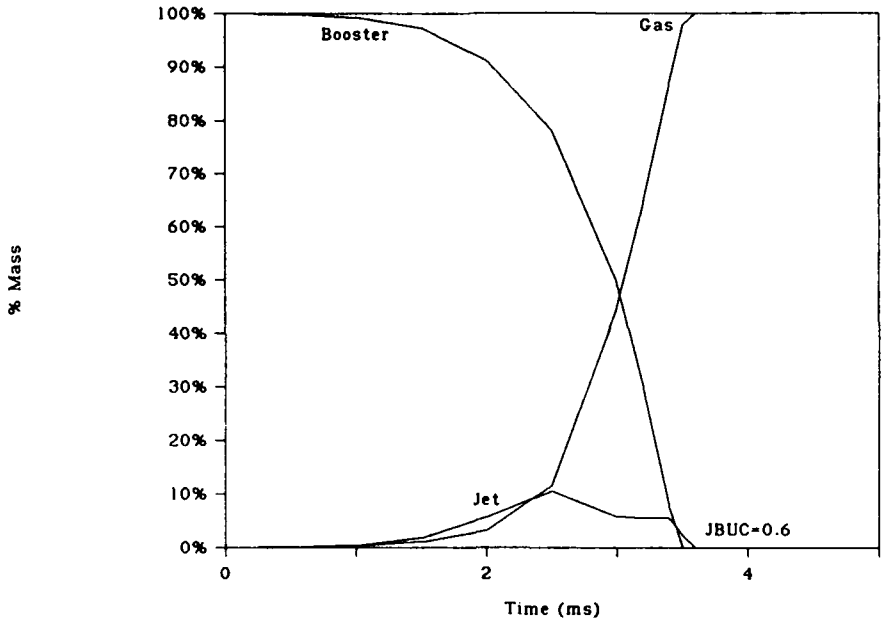

Figure 4. Percent Mass in Booster, Jet and Gas for JBUC=0.6.

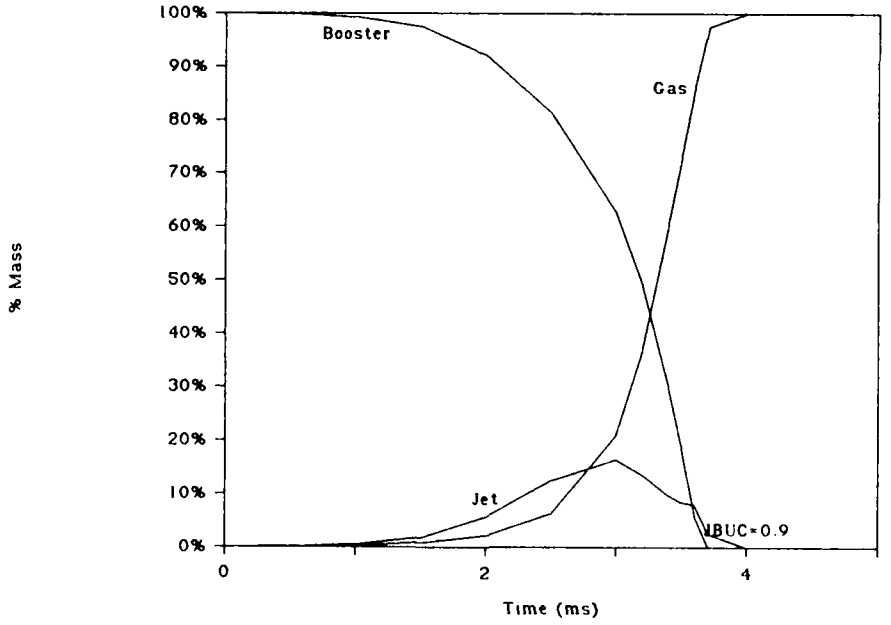

Figure 5. Percent Mass in Booster, Jet and Gas for JBUC=0.9.

portion of the cycle. "Large" JBUCs, from 0.8 to 0.9, refer to coefficients in which the jet extends into the tube for much of the ballistic cycle. These categories of JBUCs will vary for different bore sizes and gun geometries.

5. EFFECT ON PERFORMANCE

In the study, jet breakup coefficients from 0.1 to 0.9, in increments of 0.1, were examined to determine the effect on performance. The results for the various JBUCs show a progression in pressures and velocity, and, for simplicity, representative values of small, moderate and large JBUCs, namely, 0.2, 0.6 and 0.9 are discussed here. The maximum liquid and chamber pressures and muzzle velocity for these JBUCs are shown in Table 2 and Figure 6 together with results from a lumped parameter simulation using a model developed by Gough.[1] The lumped parameter representation is utilized for the liquid reservoir and combustion chamber; however, the model is one-dimensional in the tube. Instantaneous burning of injected propellant was chosen as a model option. Since the one-dimensional simulation reports a gradient in the pressures in the liquid reservoir and combustion chamber, average pressures are reported in Table 2 to allow comparison with the lumped parameter case. As a general observation the performance is within 12% in terms of maximum chamber pressure, 15% for maximum liquid pressure and within 4% in terms of muzzle velocity for the three jet lengths and the lumped parameter case shown.

Compared to the lumped parameter simulation, the short jet case has lower maximum chamber and liquid pressures with approximately the same muzzle velocity. A comparison of Figure 7 for the chamber pressure-time curves for the lumped parameter case and JBUC=0.2 shows that the short jet has a slower startup due to the delayed energy release, but that the rise rates of the two curves are similar. Chamber pressure in the diagram has been taken to correspond to pressure in the first cell of the combustion chamber near the piston face, and some pressure waves are evident in the figure. One would expect the short jet solution to be close to the instantaneous combustion solution. The presence of the jet has simply modulated the energy release which is reflected in the difference at maximum pressure. Figure 8 shows a comparison of the liquid pressure-time curves for the lumped parameter and jet cases with end of stroke indicated by the drop in liquid pressure to zero. Liquid pressure is taken at the rear position of the reservoir. The liquid pressures for the lumped parameter and short jet case follow the chamber pressure results with the maximum liquid and chamber pressures occurring at about the same time. The chamber pressure responds to the end of liquid injection by dropping rapidly as the projectile accelerates and the gas expands.

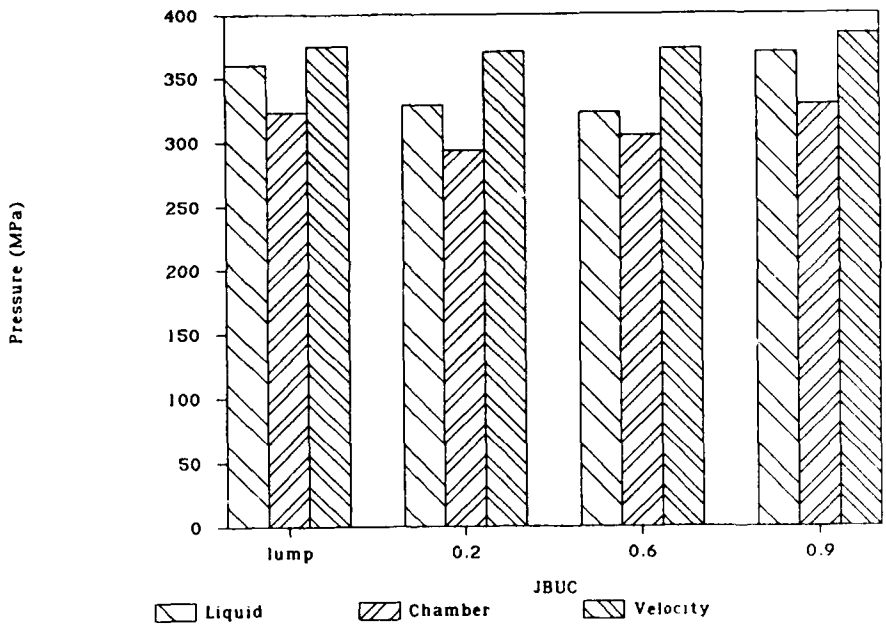

Figure 6. Maximum Liquid and Chamber Pressures and Muzzle Velocity for JBUC=0.2, 0.6, 0.9 and for Lumped Parameter Simulation.

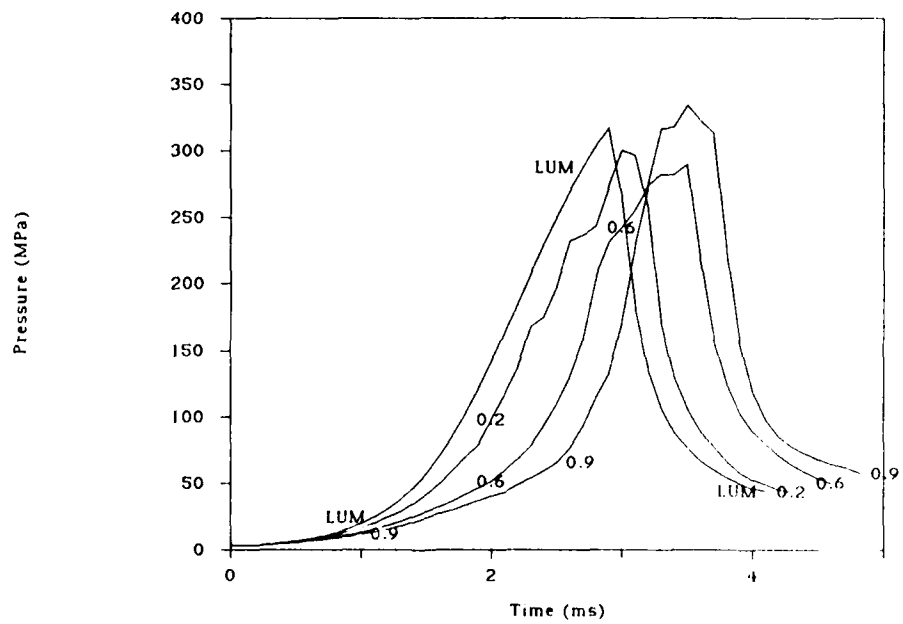

Figure 7. Chamber Pressures vs. Time for JBUC=0.2, 0.6, 0.9 and for Lumped Parameter Simulation.

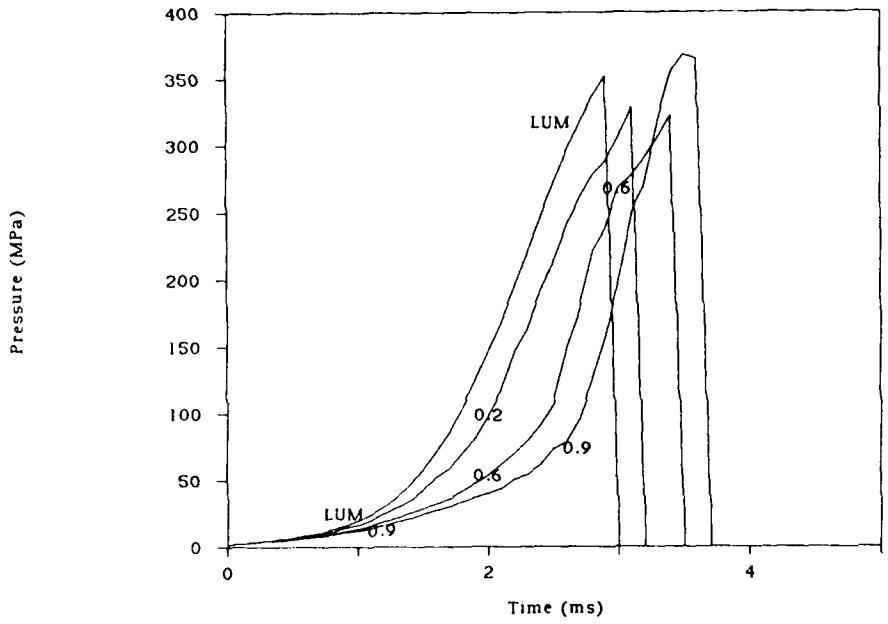

Figure 8. Liquid Pressures vs. Time for JBUC=0.2, 0.6, 0.9 and for Lumped Parameter Simulation.

Table 2. Maximum Liquid and Chamber Pressures, End of Stroke and Muzzle Velocity for JBUC=0.2, 0.6, 0.9 and for Lumped Parameter Simulation.

Jet Breakup Length (-)	Max Average Cham Pressure (MPa)	Max Average Liq Pressure (MPa)	Muzzle Velocity (m/s)	End of Stroke (sec)
Lumped Par	323.2	360.2	1499	3.0
0.2	293.6	328.5	1482	3.2
0.6	305.2	322.4	1490	3.5
0.9	328.7	369.4	1535	3.7

The JBUC of 0.6 represents a moderate jet which extends through the chamber and is occasionally in the tube. Figure 7 shows the delay in energy release in the longer startup regime. The chamber pressure curve is flatter near the peak pressure indicating more evenly distributed energy release than the lumped parameter and short jet cases. The maximum chamber pressure is also slightly lower. The liquid pressure in Figure 8 again follows the chamber pressure.

As the jet lengthens and extends into the tube for much of the ballistic cycle, as for JBUC=0.9, maximum pressures and muzzle velocity are higher than any of the other cases. The large jet breakup coefficient in the model results in slower disintegration of the jet. Since the longer jet is delivering energy locally in the tube, there is a reduced demand in the tube for gas for a long jet compared to short and moderate jets confined primarily to the combustion chamber. Thus, the higher maximum chamber pressure for large JBUCs shown in Figure 7 may reflect the reduced demand for gas from the combustion chamber. However, since liquid propellant in the tube is supplying energy, the projectile velocity is increased. The blocking of the tube by liquid is not felt to influence the pressures since some area for gas flow is available.

Although the predicted chamber and liquid pressures for a long jet are somewhat higher than the lumped parameter simulation with instantaneous propellant combustion, there is a modest benefit from the long jet in terms of predicted muzzle velocity. The muzzle velocity predicted by the lumped parameter simulation is 1499 m/s while that predicted for a JBUC of 0.9 is 1535 m/s, a 2.3% increase. On the other hand, a JBUC of 0.6 has nearly an equivalent muzzle velocity to the lumped parameter case, 1490 m/s and 1499 m/s, respectively. However, the maximum liquid and chamber pressures are lower by 11% and 6%, respectively. Hence, on the basis of this data, it appears that consideration of a liquid jet affects predicted performance in the sense that a given muzzle velocity may be attained at a lower maximum pressure than predicted by a lumped parameter simulation.

However, another comparison between the lumped parameter and the one-dimensional models is pertinent. It may be speculated that delayed combustion in the lumped parameter model in the form of droplets might yield results similar to the short and moderate jet cases. Shown in Table 3 are the results from lumped parameter simulations assuming that the injected liquid propellant breaks into droplets of the given size. The results show that the case with small droplets of 8 microns is closest in pressures to the JBUC of 0.2. A comparison of the chamber pressures for the lumped parameter case with droplets and the short jet with JBUC of 0.2 is shown in Figure 9. The pressure histories are seen to be similar, but the muzzle velocities differ by a maximum of 3.6%.

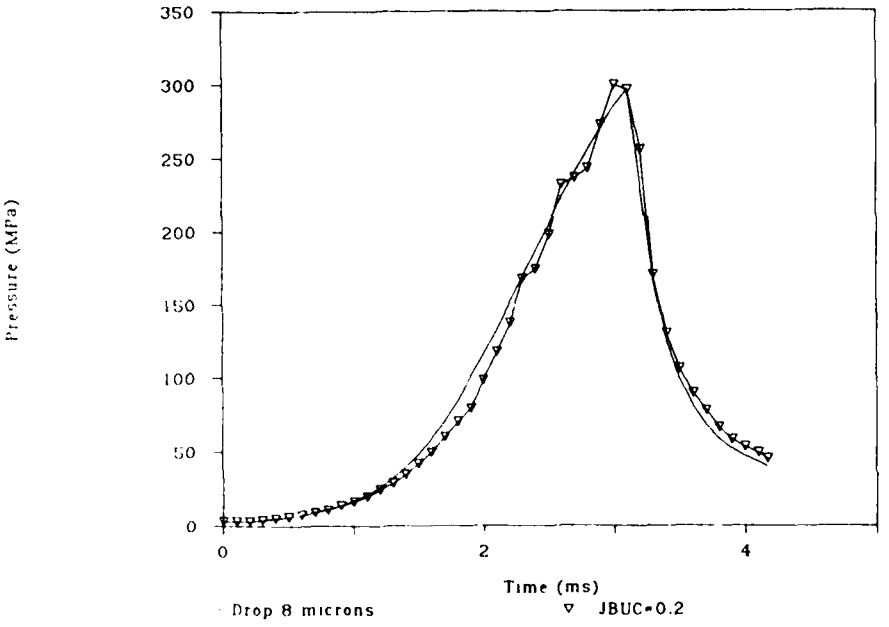

Figure 9. Chamber Pressure vs. Time for JBUC=0.2 and for Lumped Parameter Simulation with Droplets of 8 Microns.

Table 3. Maximum Liquid and Chamber Pressures, and Muzzle Velocity for Lumped Parameter Simulations Assuming Droplets.

Lumped Parameter Droplet Size (microns)	Maximum Chamber Pressure (MPa)	Maximum Liquid Pressure (MPa)	Muzzle Velocity (m/s)
5	310.8	345.2	1454
8	297.4	330.2	1428
50	208.4	230.1	1239
100	162.6	178.8	1144

Although the difference is not large, it is on the same order as the difference in velocity between the lumped parameter representation with instantaneous burning and the one-dimensional model of the jet shown in Table 2. Since the gun considered does not have chambrage and the difference in area between the chamber and the bore is large, geometric considerations in the one-dimensional model are not expected to be a major contributor to the differences in velocity. The differences may be due to the consideration of the momentum of the jet in the one-dimensional simulation and differences in the computed sound speed between the two models. Based on these results, it appears that a consideration of the liquid jet in the one-dimensional model is not analogous to delayed combustion in the lumped parameter model in the form of droplets.

In general, although jet breakup length affects the predicted performance of the RLPG compared to a lumped parameter simulation, at least for the small caliber 25-mm gun under consideration, its effect does not appear to be significant. In the opinion of the authors, predicted pressures within 10% in the range of 300 MPa, are not significantly different, especially considering a numerical error of 1 - 3%. For jets confined primarily to the chamber, as the jet lengthens the maximum liquid and chamber pressures decrease and muzzle velocity increases moderately compared to the lumped parameter case. As the jet length increases further to permit a slowly disintegrating jet which extends into the tube, maximum liquid and chamber pressures rise and muzzle velocity increases. Thus, jets confined primarily to the combustion chamber are associated with improved performance in terms of pressures (equivalent velocity at lower pressures compared to a lumped parameter model), while longer jets are associated with improved performance in terms of muzzle velocity. The results indicate that lumped parameter codes may result in overestimation of maximum gun pressures for cases with liquid jets in the chamber as a result of the predicted pressure drop from the chamber to the tube. However, both the lumped parameter and the one-dimensional model predict gun operation in the same regime of pressure and velocity.

Perhaps contrary to intuition, this result argues against a ballistic advantage of extended liquid jets in a regenerative liquid propellant gun. The presence of a jet affects the progressivity or energy release of the propellant. In the case of jets, the jet consists of unburned propellant or "stored" energy. Compared to instantaneous combustion, the result is a modulation of the burning rate. Since the energy release is spread over a longer period of time in the case of extended jets compared to instantaneous combustion, and the projectile is further downtube, the result is nearly equivalent performance. It is also noted that even when the jet does extend into the tube, the depth of penetration is only several calibers; longer jets result in the tube entrance filling with liquid.

6. EFFECT ON PRESSURE GRADIENT

Although the consideration of a liquid jet is shown to have only a moderate impact on gun performance, the jet simulation significantly affects the predicted pressure gradient in the gun. The pressure gradient is described in this discussion as the ratio of breech pressure to projectile base pressure versus time. Shown in Figures 10, 11, 12 and 13 are plots of the ratio of breech pressure to projectile base pressure versus time for the lumped parameter simulation and for JBUCs of 0.2, 0.6 and 0.9. For the purposes of this paper, breech pressure in the one-dimensional simulation refers to the pressure reported in the first cell in the combustion chamber at the face of the piston. Thus, if breech and base pressure are equal, the ratio is 1.0, with values less than 1.0 indicating that the base pressure is greater than the breech pressure.

The basic features of the graphs are similar. Until projectile motion begins at about 1.0 ms breech pressure is equal to the base pressure. The breech pressure is higher than the base pressure during injection of the propellant with the maximum value of the ratio occurring near end of stroke in the lumped parameter case and for JBUCs of 0.2 and 0.6. In the case of the long jet the maximum value of the ratio occurs at a mid-stroke position. Liquid in the tube then supplies pressure locally, causing the base pressure, and the ratio of breech to base pressure to fall. After the injection process is completed, the ratio of breech to base pressure decreases to 1.0, and rarefaction wave results in a base pressure higher than the breech pressure. The curve terminates at projectile exit. Although the curves are similar, the pressure gradients differ in the timing of events since, as the jet lengthens, the energy release is slower. Also, the gradient for a JBUC of 0.6 in comparison with the chamber pressure curve in Figure 7 indicates that around 3.0 ms the base pressure rises more than expected. The rise in base pressure can be correlated with the intrusion of the jet into the tube for a short time.

A comparison of Figures 10 and 11 shows that the pressure gradients for the lumped parameter simulation assuming instantaneous combustion and for the short jet are similar. Since combustion occurs and chamber pressure rises until end of stroke in both simulations, it is expected that a rarefaction wave will be launched when the energy supply in the chamber is exhausted, corresponding to the peak at about 3.0 ms. Consider the sound speed in a non-ideal gas,

$$c = \sqrt{\frac{\sigma P}{\rho(1 - b\rho)}}$$

where σ is the ratio of specific heats, ρ is the gas density, b is the covolume, P is pressure and c

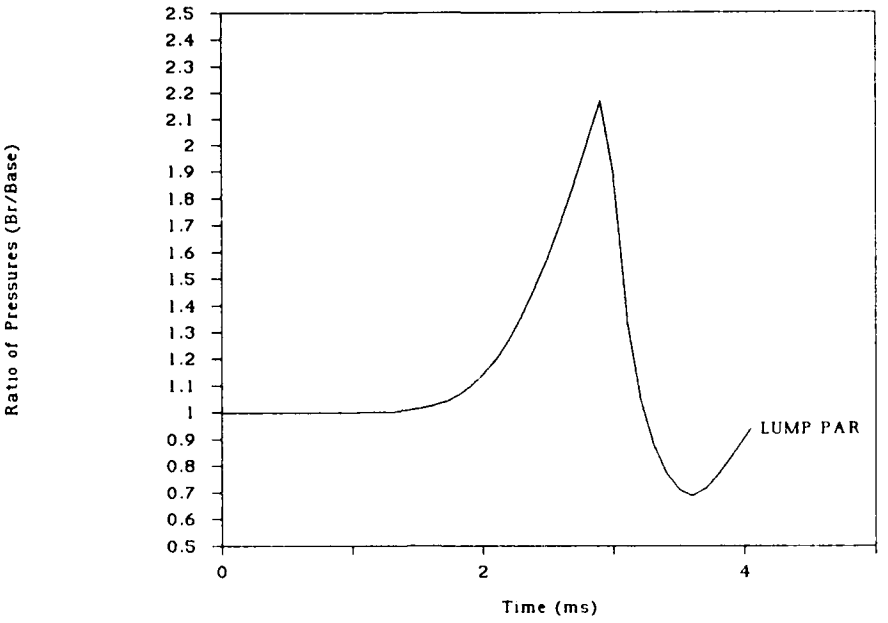

Figure 10. Ratio of Breech Pressure to Projectile Base Pressure for Lumped Parameter.

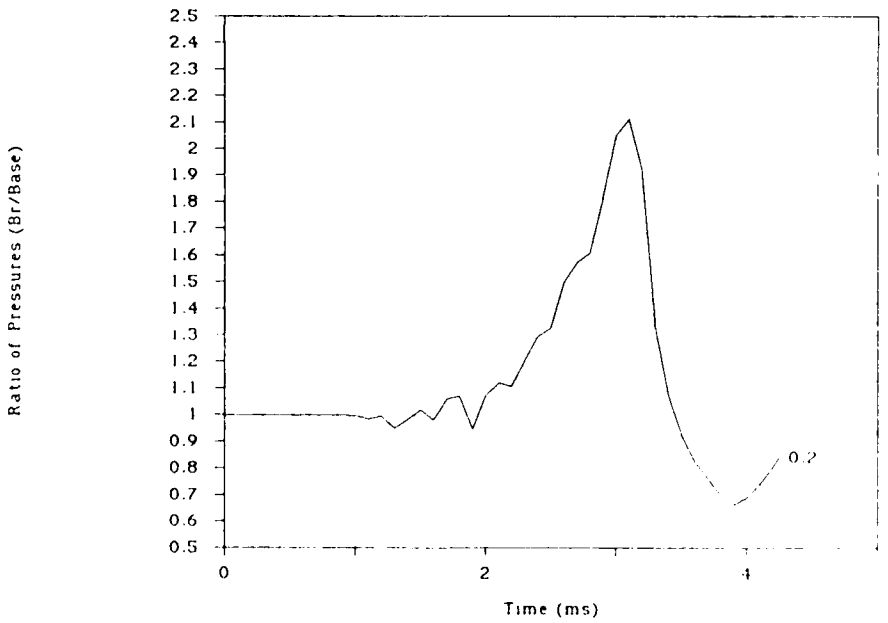

Figure 11. Ratio of Breech Pressure to Projectile Base Pressure for JBUC=0.2.

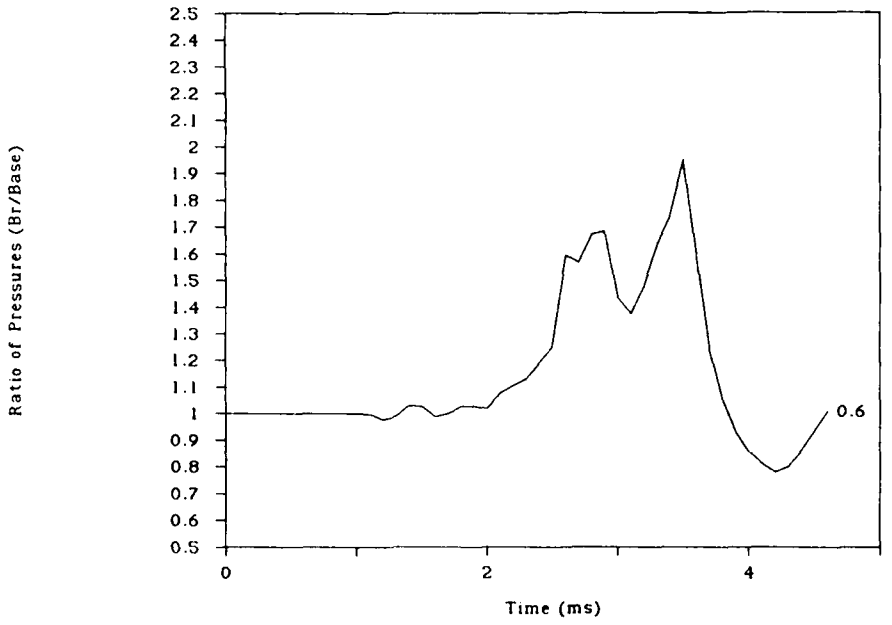

Figure 12. Ratio of Breech Pressure to Projectile Base Pressure for JBUC=0.6.

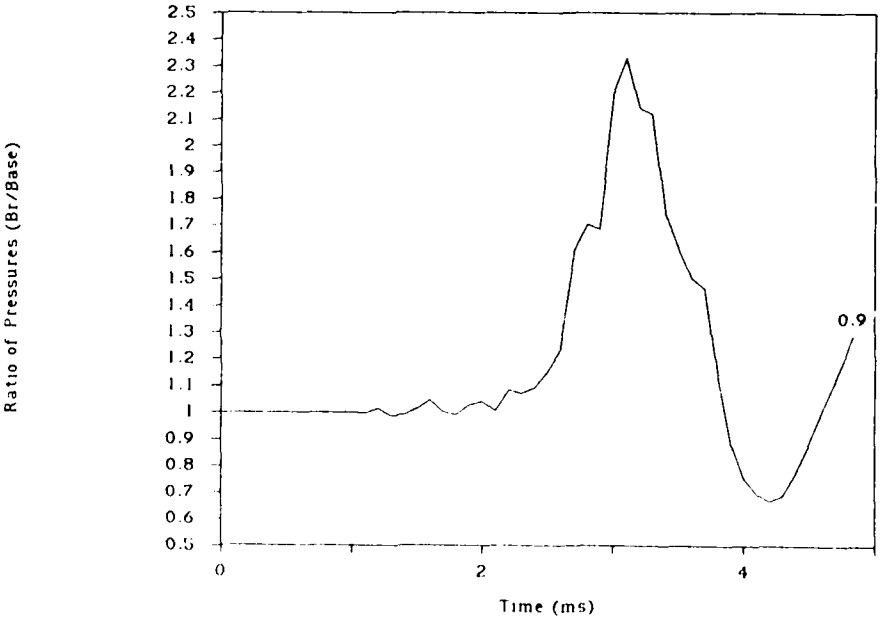

Figure 13. Ratio of Breech Pressure to Projectile Base Pressure for JBUC=0.9.

is the sound speed. An estimation of the sound speed near end of stroke for JBUC of 0.2, a case where the jet disintegration is rapid and, therefore, nearly all gas at end of stroke, is approximately 145,000 cm/s. Recognizing that the sound speed is constantly varying, this value would predict 0.9 ms for a wave to move from the breech to the projectile base for a JBUC of 0.2. The time lapse from the large peak at 3.1 ms for a JBUC of 0.2 to the minimum of the ratio at 3.9 ms is 0.8 ms. Considering the approximation, the agreement is reasonable.

The major difference between the pressure gradients for the lumped parameter case and for the short jet is the timing of events. End of stroke, and, hence, of the declining ratio of pressures, occurs 0.2 ms later for the jet case. Figures 14 and 15 are graphs of the chamber and base pressures for the lumped parameter case and for JBUC of 0.2. The figures show the difference in timing, but also the comparability of the base pressures. Thus, although the maximum chamber pressure for JBUC of 0.2 is approximately 9% lower than the lumped parameter case, the muzzle velocities are within 1%.

Although the pressure gradients for the moderate and long jets in Figures 12 and 13 also show a rarefaction wave beginning near end of stroke followed by subsequent reflection, the curves have some essential differences with those of the lumped parameter and short jet cases. The JBUC of 0.6 defines a jet which intrudes into the tube approximately 1.5 cm early in the piston stroke with about 25% of the liquid propellant injected at 2.6 ms. The predicted slow disintegration rate for liquid propellant injected early in the injection cycle leads to accumulation which burns off with about 50% of the propellant injected at 3.0 ms. Thereafter, the jet is confined to the chamber. The effect of the jet intrusion in the tube is reflected in the pressure gradient in Figure 12 from 2.5 ms to 3.5 ms.

On the other hand, the JBUC of 0.9 defines a jet which intrudes into the tube as a continuous jet from 1.4 ms with 2% of the liquid propellant injected until 3.5 ms with 82% of the propellant injected. At 3.6 ms the jet becomes fragmented, with segments of jet in the chamber and tube. Fragments of the jet continue to exist until 3.8 ms. This continuous local supply of gas in the tube reduces the demand for gas in the chamber, and the pressure gradient in Figure 13 reflects the slow disintegration rate both in the timing of events and the steeper pressure gradient, that is, higher ratio of breech to base pressure, near end of stroke.

A comparison of the chamber and base pressures for the lumped parameter simulation and for JBUCs of 0.2, 0.6 and 0.9 in Figures 14, 15, 16 and 17 demonstrates the slowing disintegration

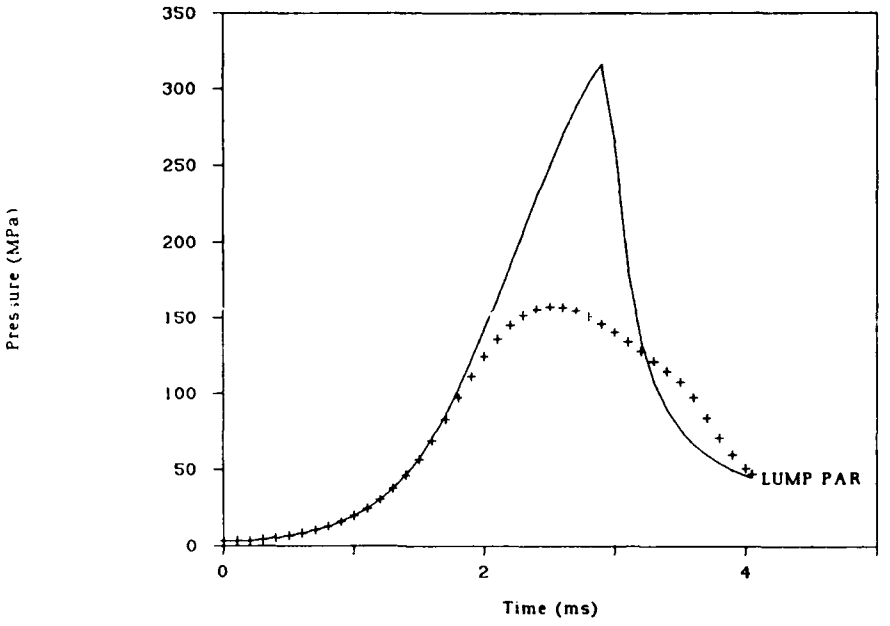

Figure 14. Combustion Chamber and Projectile Base Pressures for Lumped Parameter Simulation.

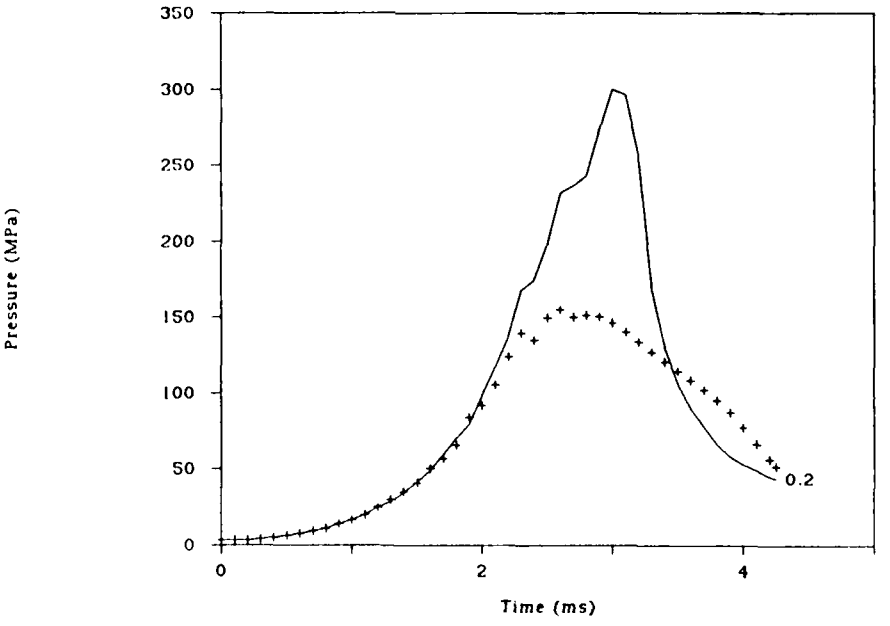

Figure 15. Combustion Chamber and Projectile Base Pressures for JBUC=0.2.

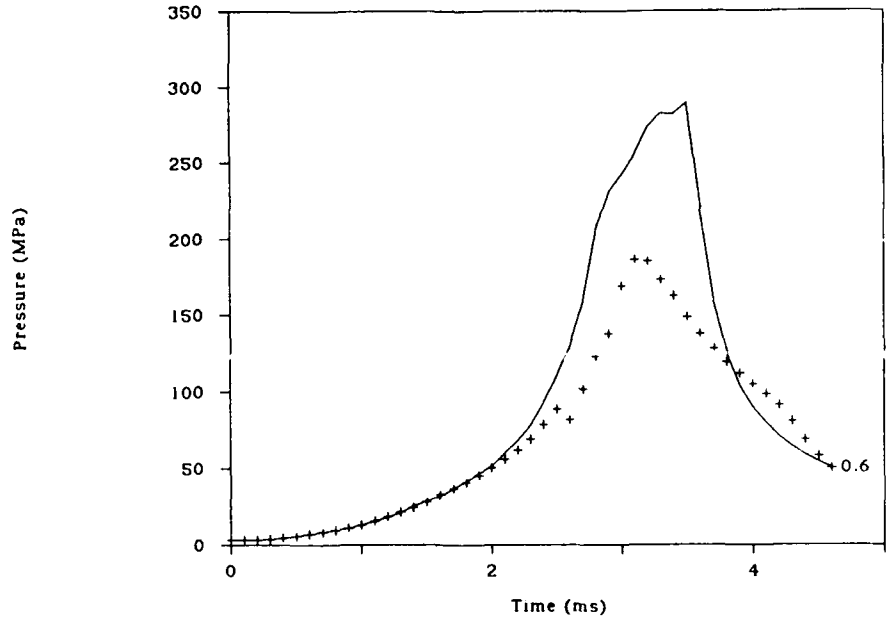

Figure 16. Combustion Chamber and Projectile Base Pressures for JBUC=0.6.

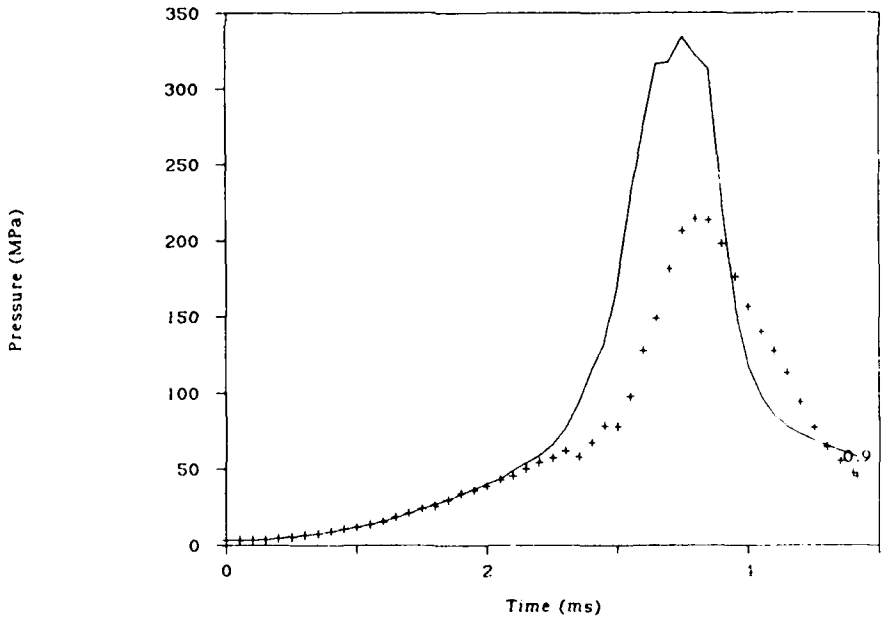

Figure 17. Combustion Chamber and Projectile Base Pressures for JBUC=0.9.

rate and, hence, energy release, of longer jets. The response of the base pressure begins to lag that of the combustion chamber. As the jet intrudes into the tube for much of the ballistic cycle, mass addition from the jet in the tube inhibits the local demand for gas. As a result of propellant in the tube, the base pressure is substantially higher for the long jet in Figure 17 than for the short jet shown in Figure 15. The higher base pressure results in muzzle velocity improvement of about 3.5% over the short jet.

In general, the consideration of a liquid jet in the regenerative liquid propellant gun introduces a variety of pressure waves. Although small amplitude waves are observed early in the interior ballistic cycle, the dominant wave action occurs at the end of stroke when liquid injection ceases. End of stroke does not necessarily correspond to burnout since ligaments of the jet may persist for some time. After injection has ceased, the chamber pressure falls below the projectile base pressure. As the jet breakup coefficient increases, the jet intrudes into the tube. In the case of long jets, local mass addition in the tube reduces the demand for gas from the combustion chamber. The jet extension into the tube, however, provides energy deposition closer to the base of the projectile maintaining the projectile acceleration.

7. EFFECT ON PRESSURE PROFILE

In lumped parameter models of the RLPG it is assumed that the momentum of the entering liquid propellant is dissipated in the combustion chamber. Early designs utilized a number of small jets in a shower head arrangement making this assumption reasonable. However, current designs employ a single, annular jet which may persist for some time in the chamber and possibly in the tube. Therefore, it is hypothesized that the pressure drop between the combustion chamber and gun tube may be less than that predicted by lumped parameter models. Thus, the purpose of this section is to explore the relationship between the breech pressure, defined as above as the pressure at the rear of the combustion chamber, and the throat pressure for various jet breakup coefficients and to compare the results to a lumped parameter simulation.

The effect of a representation of a jet on the relationship between breech and throat pressure can be quantified by the ratio of breech pressure to throat pressure. Figure 18 is a graph of the ratio of breech pressure to throat pressure (Br/Throat) versus time for a lumped parameter simulation. The projectile begins moving at about 1.0 ms after which the ratio between breech and throat pressure increases to approximately 1.45 at maximum breech pressure. A comparison with Figure 19 for a short jet shows an expected unevenness in the ratio since the energy supply is uneven, but overall similarity with the lumped parameter case.

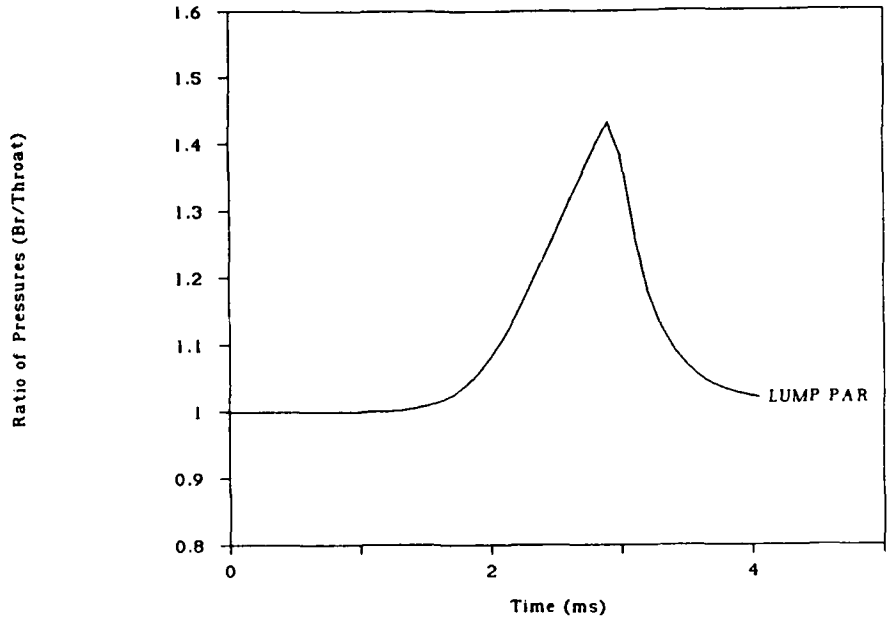

Figure 18. Ratio of Breech Pressure to Throat Pressure for Lumped Parameter Representation.

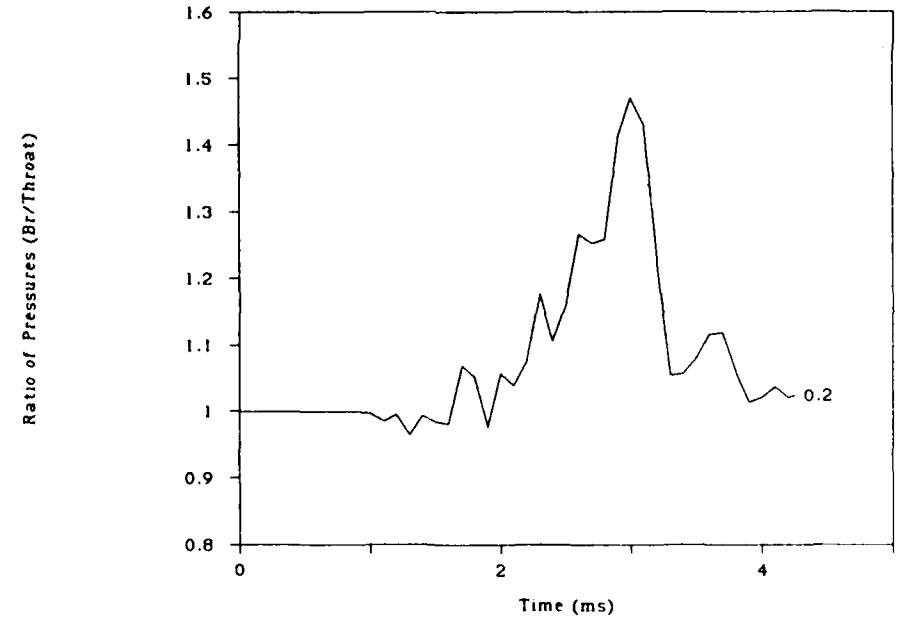

Figure 19. Ratio of Breech Pressure to Throat Pressure for JBUC=0.2.

In contrast, as the jet lengthens to extend into the tube, the ratio of breech to throat pressure does not generally increase over the injection cycle as seen in Figure 20 for a moderate jet and Figure 21 for a long jet. Although the jet extends only several centimeters into the tube for the moderate jet during the early injection part of the cycle and almost continuously into the tube for long jet, the effect at the throat is similar. That is, a large pressure drop is not observed at the throat while the jet is present from 1.3 to 2.5 ms for JBUC=0.6 and from 1.4 to 3.5 ms for JBUC=0.9, and the ratio of pressures is nearly one. The spike in the ratio of breech to throat pressures for both the moderate and long jet around 2.5 ms occurs as the throat becomes nearly filled with liquid. The flow area is small, and the gas velocity at the throat becomes large with a corresponding drop in throat pressure. Thus, since the breech pressure is increasing at this point, the ratio becomes large. However, the system equilibrates again, and a ratio near one is re-established. Near end of stroke as the supply of liquid propellant is slowed, the throat pressure drops, and the ratio increases.

The results shown in the preceding figures do not, however, complete the description of the pressure distribution. A pressure drop does occur in the gun in the case of moderate and long jets. However, the drop in pressure is associated with the leading edge of the liquid jet in the tube. Shown in Figures 22 and 23 are the pressure and gas velocity gradients in the tube for a lumped parameter representation at 2.5 ms with approximately 50% of the propellant injected and at a projectile travel of 34.47 cm. The zero is the entrance to the tube, with the state of the gas in the combustion chamber indicated to the left of the zero. Since the lumped parameter model assumes that the gas in the chamber is stagnant, the gas velocity is zero to the left of the tube entrance in Figure 23. The curves show the Lagrange gradient assumed in the model. By comparison, the pressure and velocity gradients for a long jet at 3.2 ms, 50% of propellant injected, and projectile travel of 32.66 cm shown in Figures 24 and 25 show the effect of the presence of the jet. The jet extends 3.27 cm into the tube, and its presence is reflected by a drop in pressure across the jet to the leading edge and a corresponding increase in gas velocity.

Thus, even with a liquid jet, there is a pressure drop in the gun. However, the location of the drop in pressure may not be located at the throat in the case of an extended jet. In the ideal situation characterized by complete combustion of the injected propellant within the chamber, a large mass flux will occur at the entrance to the tube in order to compensate for the motion of the projectile. Since the gas in the combustion chamber will be essentially at rest, the flow into the tube will be accompanied by a pressure drop. If, instead of the ideal situation, distributed combustion is allowed due to the finite breakup length of the jet, and if the jet is sufficiently long

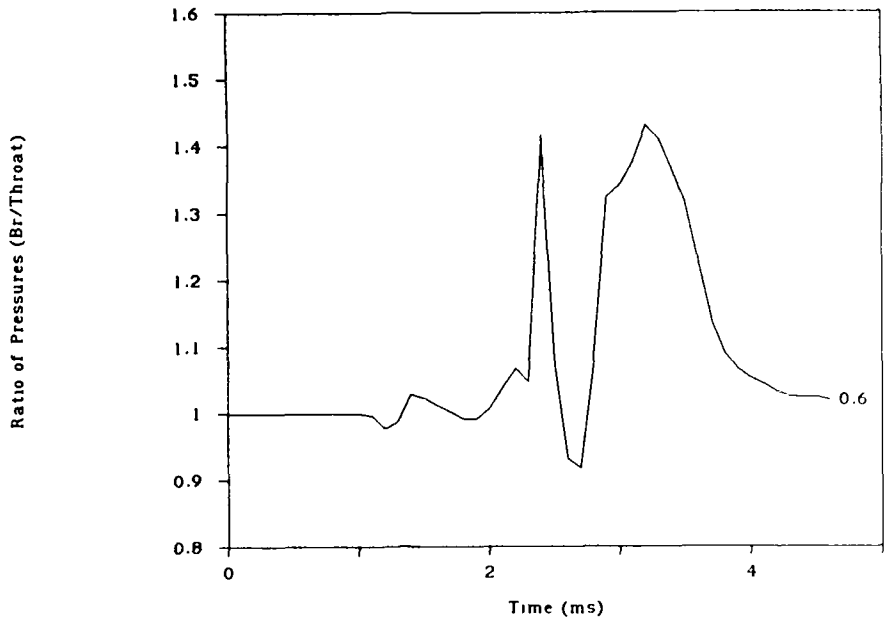

Figure 20. Ratio of Breech Pressure to Throat Pressure for JBUC=0.6.

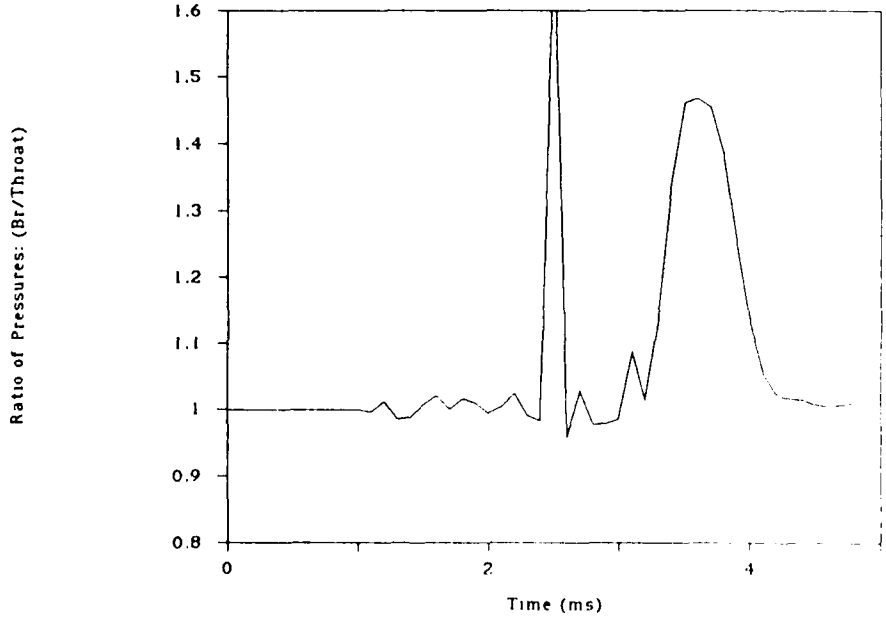

Figure 21. Ratio of Breech Pressure to Throat Pressure for JBUC=0.9.

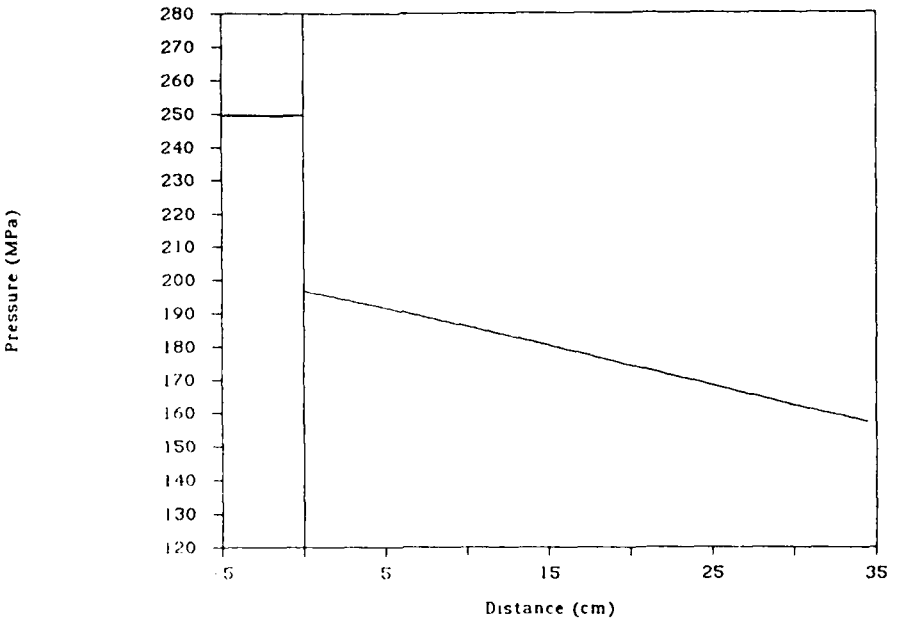

Figure 22. Pressure Gradient in the Tube for Lumped Parameter Representation at 50% Propellant Injected and 34.47 cm Projectile Travel.

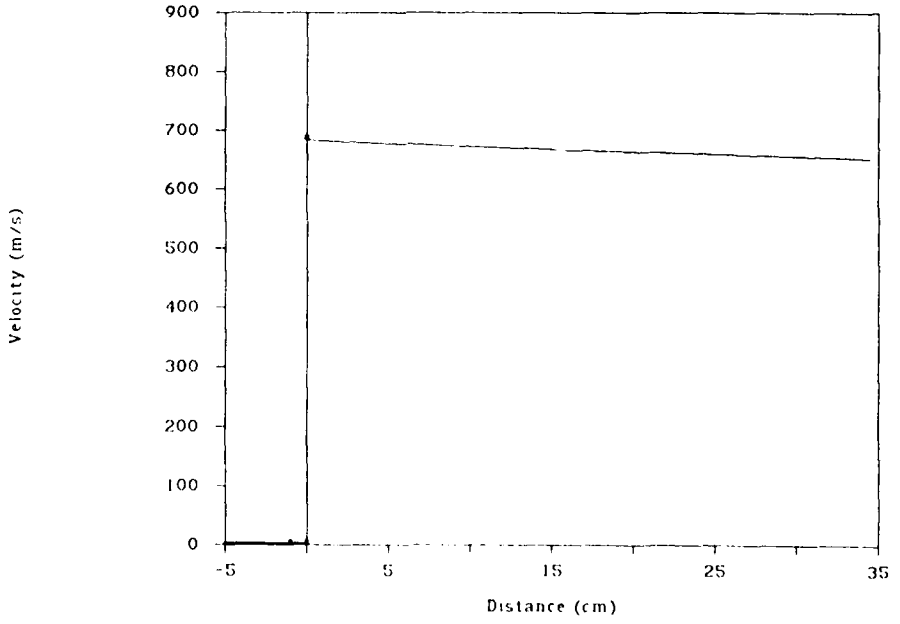

Figure 23. Velocity Gradient in the Tube for Lumped Parameter Representation at 50% Propellant Injected and 34.47 cm Projectile Travel.

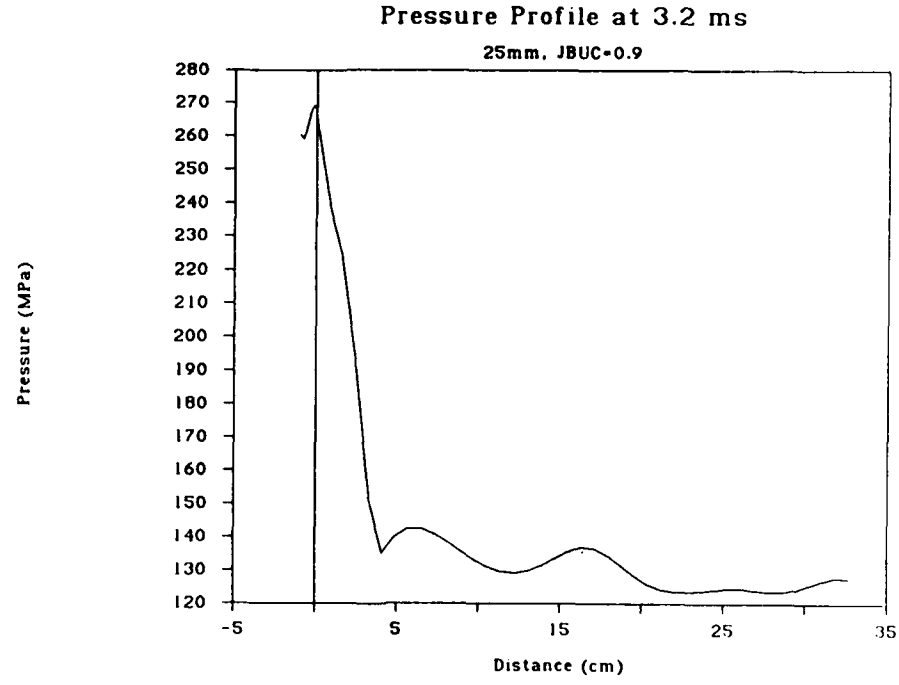

Figure 24. Pressure Gradient in the Tube for JBUC=0.9 at 50% Propellant Injected and 32.66 cm Projectile Travel.

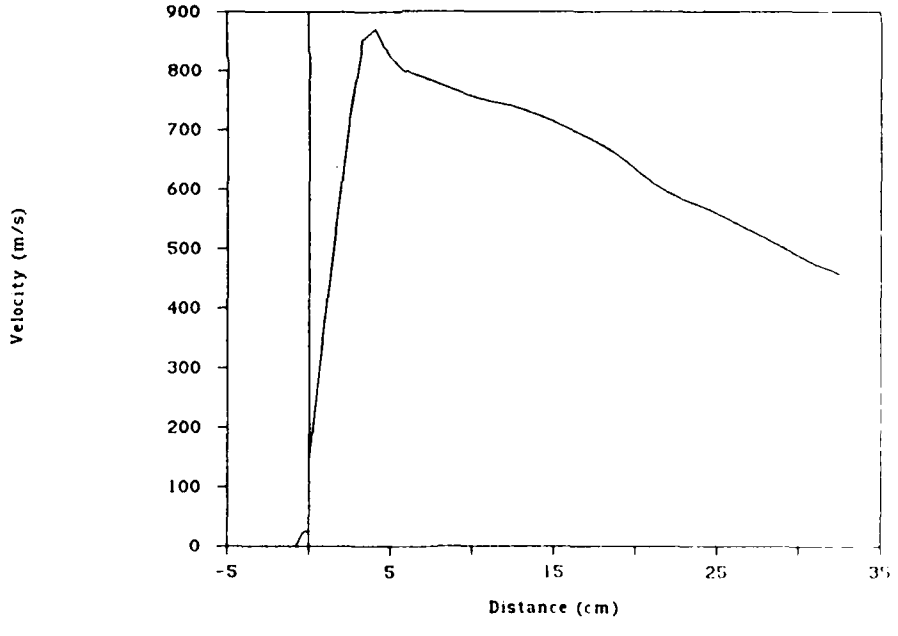

Figure 25. Velocity Gradient in the Tube for JBUC=0.9 at 50% Propellant Injected and 32.66 cm Projectile Travel.

to provide a source of combustion energy within the tube itself, the rate of pressurization within the tube may be sufficient to compensate for the projectile motion and to maintain equilibrium with the conditions in the chamber. Clearly, this condition will only apply to the part of the tube into which the jet intrudes. Forward of the jet, demand for pressurization will occur and the pressure drop seen ideally at the entrance of the tube is now observed at a location downbore. If the combustion chamber is visualized as the region of the gun in which the energy is released, then the jet can be viewed as a mechanism which extends the combustion chamber. Hence, the jet representation permits a dynamic shape to the chamber, varying with the jet length. The stagnation of the flow in the chamber which occurs ideally is replaced by a condition of stagnation over a region of varying geometry which includes part of the tube. The condition of extended stagnation is a consequence of a continuous exchange of acoustic information throughout the region occupied by the jet. Some mass exchange occurs during the period when the jet intrudes into the tube, but it is much smaller than that which would occur under ideal conditions.

The presence of the jet implies, then, that there may not necessarily be a large pressure drop between the chamber and the tube entrance. The pressure drop from the combustion chamber to the tube for the lumped parameter simulation shown in Figure 22 is 60 MPa. The pressure drop associated with the long jet in Figure 24 is 2 MPa from the chamber to the throat. Thus, the pressure drop from the combustion chamber to the tube may be overestimated by the lumped parameter model in cases in which extended jets are present.

The effect of the jet on the pressure and velocity gradients is significant from two perspectives. First, estimates of tube thickness and resulting gun mass are based upon expected pressures and temperatures. If the pressure drop between the combustion chamber and gun tube are over-estimated, estimates of required tube thickness will be inaccurate. On the other hand, in the case of an extended jet the pressure in the tube will be higher then in the ideal situation. Heat transfer and wear characteristics will also be affected by the relocation of the region of maximum convection. Secondly, experimental data from RLPGs should be viewed with consideration given to the presence of a jet. Analysis of firing data, especially pressure differences between gages, should be viewed with the concept of a jet in mind. Differences in the tube gages may be reflective of the intrusion of a jet. On the other hand, if a jet is believed to intrude into the tube, pressure gages may be located to determine jet length from pressure histories.

8. EFFECT ON LIQUID ACCUMULATION

An important factor in RLPG operation is liquid accumulation in the combustion chamber and possibly in the tube. Estimates of accumulation are usually derived from experimental data by comparing the amount of liquid propellant injected (determined by the direct measurement of piston position) to the liquid propellant energy released (as measured by pressure and projectile motion). Estimates have ranged as high as 40% for some guns and regimes of the RLPG. Accumulation is usually conceptualized as a cloud of dispersed droplets which may be totally or partially decomposed. It seems likely that a model of a liquid jet would also exhibit this feature, especially for longer jet breakup coefficients when the jet is disintegrating slowly. In an effort to quantify and compare accumulation between various jet lengths, the following data are presented.

One measure of accumulation is the departure from the steady state regime as shown in Figure 26 for JBUCs of 0.2, 0.6 and 0.9. Figure 26 displays the ratio of the rate of injection to the rate of disintegration of the liquid propellant versus time. The definition of steady state used here is that the rate of injection of the liquid propellant is equal to the rate of disintegration. That is, steady state in Figure 26 occurs at a value of 1.0. For values greater that 1.0, the liquid is being injected faster than it is disintegrating leading to accumulation.

All jet breakup coefficients show the initial injection of liquid as the piston begins to move at about 0.1 ms. The short jet remains closest to steady state, although some accumulation does occur. The ratio of injection to disintegration for JBUC of 0.6 shows a rate of injection about 2.5 times the rate of disintegration for the early portion of the injection cycle. As the JBUC increases further to 0.9, the rate of injection is substantially higher than the rate of disintegration reaching a maximum ratio of approximately 4.0, implying that a large quantity of unburned liquid propellant accumulates in the combustion chamber and tube. These results confirm the observations from Figures 4 and 5 in which up to 10% of the mass was seen to accumulate in the jet for a JBUC of 0.6 and 20% for a JBUC of 0.9.

A comparison with the chamber pressure-time curve for the long jet in Figure 17 shows that the increasing ratio of liquid injection to disintegration corresponds to the relatively long, slow rise in chamber pressure from 0.0 to 2.5 ms which, for this JBUC, may be categorized as the start-up regime. As the chamber pressure rapidly increases from approximately 2.5 ms to 3.5 ms in Figure 17, the ratio of injection to disintegration of liquid propellant rapidly falls in Figure 26 with the endpoint at 3.7 ms marking the end of piston motion. Thus, there is a significant amount of

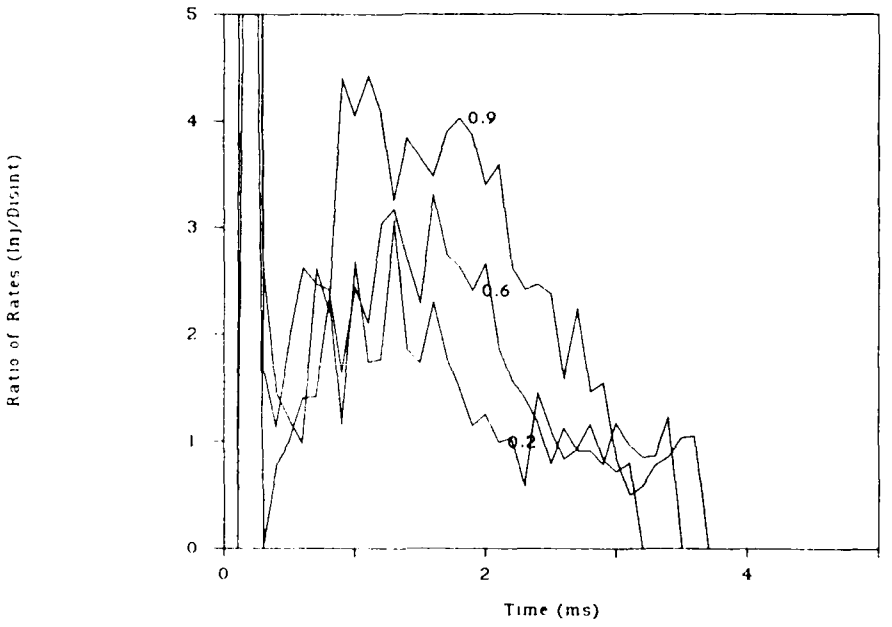

Figure 26. Ratio of Rate of Injection of Liquid Propellant to Rate of Disintegration of Liquid Propellant for JBUC=0.2, 0.6 and 0.9.

accumulation during the start-up region for a large jet breakup coefficient which is dissipated after piston motion has been established.

In general, consideration of a liquid jet can result in significant liquid accumulation in the combustion chamber and the tube for larger jet breakup coefficients. As the jet length increases, accumulation also increases. If droplets are assumed to strip from the jet and burn, the quantitative values of liquid accumulation will change to reflect an even higher liquid accumulation.

9. COMPARISON TO EXPERIMENTAL DATA

This study is intended only as a theoretical study of the predicted influence of liquid jets on the interior ballistics of regenerative liquid propellant guns. Therefore, no direct comparison with experimental data has been attempted. There is no correlation of jet breakup coefficients with the combustion process in the RLPG, and an assessment of the model's validity in the RLPG has not been established. However, it is tempting to conclude with several observations of published experimental data and the similarities to the model.

An overview of the RLPG by Morrison et al[12] describes data from a 105-mm firing of a Concept VI RLPG, a fixture similar in design to that used in the model. Figure 27 shows slightly

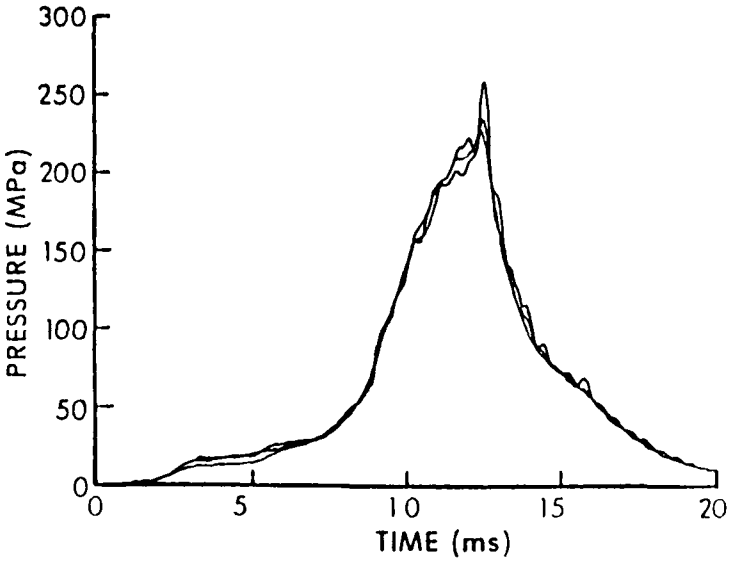

Figure 27. Experimental Combustion Chamber Pressure Data from Three 105-mm Firings of a Concept VI RLPG.

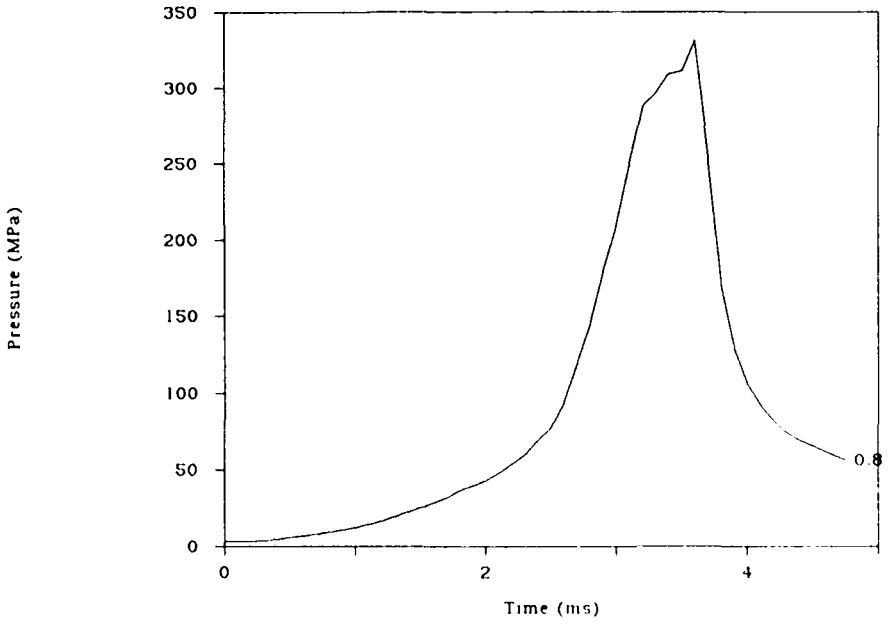

Figure 28. Simulation of Combustion Chamber Pressure for a 105-mm Gun with a Long Jet.

flattened pressure-time curves in experimental data with a distinctive peaking at maximum pressure. A simulation of a 105-mm gun shows similar pressure curves for longer jets shown in Figure 28. The distinctive shape of the pressure-time curve has not been produced by any other type of

simulation. Although the similarities are not a validation of the model, it appears that the model qualitatively describes some observed characteristics of the regenerative liquid propellant gun.

10. CONCLUSIONS

A fully one-dimensional model of a regenerative liquid propellant gun has been presented in which the liquid jet is explicitly represented. The usual modeling assumption of stagnation in the combustion chamber has been replaced by considering a liquid jet which may extend into the tube. Performance and pressure gradients have been related to the model of the jet and to the jet breakup coefficient which determines the disintegration rate of the jet. The major observations are:

1) The mass in the system can be divided into four components: booster propellant in the liquid reservoir, a liquid jet which extends into the combustion chamber and may extend into the tube, liquid droplets which are stripped from the jet, and gas. In this study only booster, jet and gas were considered. As the jet breakup coefficient increases, the jet extends further axially and contains more mass.

2) Perhaps contrary to intuition, results of the one-dimensional modeling argue against a ballistic advantage of extended liquid jets in a regenerative liquid propellant gun. Although jet breakup length modestly affects performance of the small caliber 25-mm regenerative liquid propellant gun under consideration, it is not considered to be a significant factor.

3) Consideration of a jet affects the chamber pressure history in the gun. If the jet intrudes into the tube for most of the injection cycle, the stagnation condition ideally associated with the chamber is extended into that part of the tube occupied by the jet. As a result, mass transfer at the entrance to the tube is very small by comparison with that which occurs in the ideal situation. However, the long jet deposits energy closer to the projectile base, maintaining the projectile acceleration.

4) The presence of a jet is reflected in the pressure drop between the combustion chamber and tube. The pressure drop is much less pronounced for jets intruding into the tube, particularly when compared to a lumped parameter representation. However, the pressure drop is evident further down the tube at the leading edge of the liquid jet.

5) Experimental data from RLPGs should be viewed with consideration given to the presence of a jet. Differences in the tube gages may be reflective of the intrusion of a jet.

6) As jet breakup length increases, liquid accumulation increases. In this study up to 20% of the total mass accumulates in the combustion chamber and tube as unburned liquid propellant.

7) Although no direct comparison with experiments is made, some observed characteristics of experimental data are reflected by the model.

11. REFERENCES

1. Gough, P.S., "A Model of the Interior Ballistics of Hybrid Liquid-Propellant Guns," Final Report for Task II, Contract DAAK11-82-C-0154, September, 1983.

2. Coffee, T.P., "An Updated Lumped Parameter Code for Regenerative Liquid Propellant In-Line Guns," Ballistic Research Laboratory Technical Report BRL-TR-2974, December, 1988.

3. General Electric Company Ordnance Systems Division, Pittsfield, Massachusetts, private communication.

4. Gough, P.S. "Continuum Modeling of Regenerative Liquid Propellant Guns and Hybrid Traveling Charge Systems," Final Report, Contract DAAK11-84-C-0080, September, 1988.

5. Coffee, T.P., Wren, G.P. and Morrison, W.F., "A Comparison Between Experiment and Simulation for Concept VIC Regenerative Liquid Propellant Guns: I. 30 mm," Ballistic Research Laboratory Technical Report in press, 1989.

6. Coffee, T.P., Wren, G.P. and Morrison, W.F., "A Comparison Between Experiment and Simulation for Concept VIC Regenerative Liquid Propellant Guns: II. 105 mm," Ballistic Research Laboratory Technical Report in press, 1989.

7. Wren, G.P., Coffee, T.P., and Morrison, W.F., "A Comparison Between Experiment and Simulation for Concept VIC Regenerative Liquid Propellant Guns: III. 155 mm," Ballistic Research Laboratory Technical Report in press, 1989.

8. Birk, Avi, and Reeves, Phil, "Annular Liquid Propellant Jets - Injection, Atomization and Ignition," Ballistic Research Laboratory Technical Report BRL-TR-2780, March, 1987.

9. Macken, N.A., "Droplet Formation for Liquid Monopropellant Jets," Ballistic Research Laboratory Technical Report BRL-TR-2848, 1987.

10. Faeth, G.M., "Combustion Properties of High-Pressure Liquid Monopropellant Sprays," ARO-BRL-JANNAF Workshop on Liquid Monopropellant Spray Ignition and Combustion in a Gun Environment, 1986.

11. Newman, J.A. and Brzustowski, T.A., "Behavior of Liquid Sprays at High Pressure," AIAA Paper 70-8, 1970.

12. Morrison, Walter, Baer, P., Bulman, M., and Mandzy, J., "The Interior Ballistics of Regenerative Liquid Propellant Guns," Ballistic Research Laboratory Technical Report BRL-TR-2857, October, 1987.

INTENTIONALLY LEFT BLANK.

APPENDIX A:

INPUT FOR LUMPED PARAMETER CODE

INTENTIONALLY LEFT BLANK.

SIMULATION OF INTERIOR BALLISTICS OF HYBRID LIQUID PROPELLANT GUN
VERSION OF JUNE 20, 1985

25MM, INLINE, OTTO II, LUMPED PARAMETER

OPTION SWITCHES

NRGEN(0=CONVENTIONAL RLPG,1=REVERSE ANNULAR)	2
(2=CONV. COMPOUND,3=RAP COMPOUND)	
KIN1(0=INFINITE HELMHOLTZ MIXING RATE,	
1=FINITE RATE	
2=FINITE RATE,FINITE BOOSTER JET)	0
KIN2(0=INSTANTANEOUS DROPLET COMBUSTION,	
1=FINITE RATE)	0
ICP (0 - USE VENT AREA)	
(1 - COMPUTE VENT AREA FOR CONST. PRES.)	
(2 - COMPUTE VENT AREA FOR CONST. ACC.)	0
IPAR (0 - NORMAL INPUT)	
(1 - COMPUTE LIQUID & COMBUSTION VOLUMES)	
(2 - COMPUTE LIQUID VOLUME FROM C/M)	0
NHTW (0 - WALL TEMP. NOT UPDATED	
(1 - WALL TEMP. UPDATED)	0
JHTW (0 - NO HEAT LOSS)	
(1 - HEAT LOSS TO TUBE)	1
NTEM (NO. OF TUBE INITIAL TEMP. PROFILE ENTRIES	0
NENV (NO. OF TUBE INTERVALS FOR PRESS ENVELOPE)	0
NPISR (0 - NO PISTON RESISTANCE	
(1 - PISTON RESISTANCE FUNCTION OF TRAVEL	
(2 - PISTON RESISTANCE FUNCTION OF VELOCITY	0
NCD (0 - CD IS CONSTANT)	
(1 - CD IS FUNCTION OF PISTON TRAVEL)	0
NORVS (0 - NO BACKFLOW TO LP BOOSTER CHAMBER)	
(1 - BACKFLOW IS ALLOWED)	0
IGNITR (0 - BOOSTER IGNITER NOT MODELED)	
(1 - BOOSTER IGNITER IS MODELED)	0
IGNLOC (0 - BOOSTER IGNITER NOT ON SIDEWALL)	
(1 - BOOSTER IGNITER IS ON SIDEWALL)	0
NXPEL (0 - TC EXPULSION CHARGE NOT PRESENT)	
(1 - TC EXPULSION CHARGE IS PRESENT)	0
NARB (0 - VENT GEOMETRY NOT PRESCRIBED BY ARBV 0)	
(1 - VENT GEOMETRY SPECIFIED BY ARBVEN)	

LOGOUT PARAMETERS

SAVE ON UNIT 8(0=NO,1=YES)	0
START FROM UNIT 8(0=NO,>0=STEP TO START)	0
PLOTTING ON LOGOUT(0=NO,1=YES)	1
NUMBER OF STEPS BEFORE LOGOUT	9999
TIME INTERVAL BEFORE LOGOUT(MSEC)	0.100
DEBUG PRINT REQUIRED (0=NO,1=YES)	0
INPUT DATA PRINTED (Y=0,N=1)	0
TRAJECTORY DATA PRINTED (Y=0,N=1)	0

EXTRA TRAJECTORY DATA PRINTED (Y=0,N=1)	0
MASS BAL. REG 1>4 DATA PRINTED (Y=0,N=1)	0
MASS BAL. REG 5>8 DATA PRINTED (Y=0,N=1)	0
ENERGY BAL. REG 1>4 DATA PRINTED (Y=0,N=1)	0
ENERGY BAL. REG 1>4 (CONT) DATA PRINTED (Y=0,N=1)	0
ENERGY BAL. REG 5>8 DATA PRINTED (Y=0,N=1)	0
PROFILE AND PLOT DATA PRINTED (Y=0,N=1)	0

TERMINATION PARAMETERS

NUMBER OF INTEGRATION STEPS	99999
TIME INTERVAL(MSEC)	100.000
PROJECTILE TRAVEL(CM)	213.300

INTEGRATION PARAMETERS

NUMBER OF POINTS ASSIGNED TO TRAVELING CHARGE	0
MAXIMUM NUMBER OF POINTS ASSIGNED TO TUBE	41
MINIMUM MESH SPACING IN TRAVELING CHARGE(CM)	0.500
MINIMUM MESH SPACING IN TUBE(CM)	0.100
C-F-L SAFETY FACTOR(-)	2.000
FLUX CONVERGENCE TOLERANCE(GM**2/SEC**2)	0.010
SOURCE TERM STABILITY FACTOR(-)	0.050

DESCRIPTION OF TUBE

NUMBER OF PAIRS OF OBTURATOR RESISTANCE DATA	3
AIR SHOCK RESISTANCE(0=NO,1=YES)	1
TUBE DIAMETER(CM)	2.500
TUBE ENTRANCE COEFFICIENT(-)	1.000

OBTURATOR RESISTANCE

PROJECTILE TRAVEL(CM)	RESISTANCE(MPA)
0.000	10.000
0.010	5.500
213.300	5.500

PROPERTIES OF GAS IN FRONT OF PROJECTILE

INITIAL PRESSURE(MPA)	0.100
INITIAL TEMPERATURE(DEG.K)	300.000
RATIO OF SPECIFIC HEATS(-)	1.400
MOLECULAR WEIGHT(GM/GMOL)	28.960

PROPERTIES OF PROJECTILE

MASS(GM)	97.300
LOCATION OF BASE WITH RESPECT TO TUBE ENTRANCE(CM)	0.000
TRAVEL REQUIRED TO INITIATE VENTING OF TRAVELING LIQUID CHARGE(CM)	0.000
DENSITY OF AFTERBODY MATERIAL(GM/CC)	0.000
PRESSURE FOR SEPARATION OF TLC FROM BASE OF PROJECTILE(MPA)	0.000

PROPERTIES OF COMPOUND RLPG BOOSTER

INITIAL VOLUME OF FUEL CHAMBER(CC)	95.061
INITIAL VOLUME OF COMBUSTION CHAMBER(CC)	35.400
INJECTION HOLE AREA(CM**2)	4.897
NUMBER OF INJECTION HOLES(-)	1.000
INJECTION HOLE DISCHARGE COEFFICIENT(-)	0.900

PROPERTIES OF FORWARD CYLINDER

MASS OF PISTON(GM)	685.000
INITIAL VOLUME OF DAMPING LIQUID CHAMBER(CC)	0.000
VOLUME OF D.L. RECEIVER CHAMBER(CC)	0.000
FUEL SIDE PISTON AREA(CM**2)	16.504
COMBUSTION CHAMBER SIDE PISTON AREA(CM**2)	18.613
DAMPING CHAMBER SIDE PISTON AREA(CM**2)	0.000
MAXIMUM PISTON DISPLACEMENT(CM)	4.442
% OF MAXIMUM PISTON DISPLACEMENT	0.980

PROPERTIES OF CENTER CYLINDER

MASS OF PISTON(GM)	0.000
INITIAL VOLUME OF DAMPING LIQUID CHAMBER(CC)	0.000
VOLUME OF D.L. RECEIVER CHAMBER(CC)	0.000
FUEL SIDE PISTON AREA(CM**2)	0.000
COMBUSTION CHAMBER SIDE PISTON AREA(CM**2)	0.000
DAMPING CHAMBER SIDE PISTON AREA(CM**2)	0.000
MAXIMUM PISTON DISPLACEMENT(CM)	0.000
% OF MAXIMUM PISTON DISPLACEMENT	0.000

PROPERTIES OF REAR CYLINDER

MASS OF PISTON(GM)	0.000
INITIAL VOLUME OF DAMPING LIQUID CHAMBER(CC)	0.000
VOLUME OF D.L. RECEIVER CHAMBER(CC)	0.000
FUEL SIDE PISTON AREA(CM**2)	0.000
COMBUSTION CHAMBER SIDE PISTON AREA(CM**2)	0.000
DAMPING CHAMBER SIDE PISTON AREA(CM**2)	0.000
MAXIMUM PISTON DISPLACEMENT(CM)	0.000

% OF MAXIMUM PISTON DISPLACEMENT	0.000

PROPERTIES OF DAMPING LIQUID

DENSITY AT ONE ATMOSPHERE(GM/CC)	1.460
BULK MODULUS AT ONE ATMOSPHERE(MPA)	5103.500
DERIVATIVE OF MODULUS W.R.T PRESSURE(-)	8.217

COMPOUND BOOSTER CONTROL DATA

NPXSGN (0 - FUEL INJECTION AREA GIVEN AS FUNCTION OF Z-FWD MINUS Z-CENTER) (1 - FUEL INJECTION AREA GIVEN AS FUNCTION OF Z-CENTER MINUS Z-FWD)	0
NO. OF DATA TO DESCRIBE FWD CYL DAMPER VENT AREA	0
NO. OF DATA TO DESCRIBE CENTER CYL DAMPER VENT AREA	0
NO. OF DATA TO DESCRIBE REAR CYL DAMPER VENT AREA	0
NO. OF DATA TO DESCRIBE FWD CYL DAMPER DISCHARGE COEFF	0
NO. OF DATA TO DESCRIBE CENTER CYL DAMPER DISCHARGE COEFF	0
NO. OF DATA TO DESCRIBE REAR CYL DAMPER DISCHARGE COEFF	0
NPISRC(1) (0 - NO RESISTANCE FOR FWD CYL) (1 - RES. DEPENDS ON DISP.) (2 - RES. DEPENDS ON VEL. AND PRES.) (3 - COMBINATION OF 1 AND 2)	0
NPISRC(2) - RESISTANCE LAW FOR CENTER CYL	0
NPISRC(3) - RESISTANCE LAW FOR REAR CYL	0
NSIDEV (0 - RAP INJECTION AS ABOVE) (>0 - NUMBER OF SIDEWALL VENTING DATA)	0

PROPERTIES OF LIQUID FUEL

DENSITY AT ONE ATMOSPHERE(GM/CC)	1.230
BULK MODULUS AT ONE ATMOSPHERE(MPA)	1206.500
DERIVATIVE OF MODULUS W.R.T PRESSURE(-)	2.500
CHEMICAL ENERGY(J/GM)	3240.807
RATIO OF SPECIFIC HEATS OF PRODUCTS(-)	1.267
MOLECULAR WEIGHT OF PRODUCTS(GM/GMOL)	19.062
COVOLUME OF PRODUCTS(CC/GM)	1.257

INITIAL DATA

PRESSURE OF GAS(MPA)	3.400
PRESSURE OF LIQUID BOOSTER CHARGE(MPA)	2.000
PRESSURE OF LIQUID TRAVELING CHARGE(MPA)	0.000
TEMPERATURE(DEG.K)	1986.000
PRESSURE OF DAMPING LIQUID(MPA)	0.000

DESCRIPTION OF INITIAL CAVITY

NUMBER OF PAIRS OF DATA TO DESCRIBE CAVITY	0
CAVITY MECHANICALLY STABILIZED(0=NO,1=YES)	1

CROSS-SECTIONAL AREA COMBUSTION CHAMBER(CM**2)	25.5200

PISTON TRAVEL - INJECTION AREA TABLE

F. PISTON TRAVEL	PISTON TRAVEL(CM)	VENT AREA (CM**2)
0.0000	0.000	0.100000E-01
0.1000	0.449	4.89676
1.0000	4.488	4.89676

THERMAL PROPERTIES OF TUBE

INITIAL TUBE TEMPERATURE (DEG.K)	300.000
THERMAL CONDUCTIVITY (J/CM-SEC-DEG.K)	0.622100
THERMAL DIFFUSIVITY (CM**2/SEC)	0.147100
EMISIVITY FACTOR (-)	1.00000
HEAT LOSS MULTIPLIER FACTOR (-)	1.00000

TOTAL PROPELLANT WEIGHT (GM)	117.2470
TOTAL CHEMICAL ENERGY (KJ)	379.9750
BOOSTER WEIGHT (GM)	117.1088
TRAVELING CHARGE WEIGHT (GM)	0.0000000
IGNITER WEIGHT (GM)	0.1382631
LOADING DENSITY (GM/CC)	0.8987136
C/M	1.205006

INTENTIONALLY LEFT BLANK.

APPENDIX B:

INPUT FOR 1-DIMENSIONAL CODE

INTENTIONALLY LEFT BLANK.

1 SIMULATION OF INTERIOR BALLISTICS OF HYBRID LIQUID PROPELLANT GUN
VERSION OF JUNE 20, 1985

25MM, INLINE, OTTO II, JET

OPTION SWITCHES

NRGEN(0=CONVENTIONAL RLPG,1=REVERSE ANNULAR) (2=CONV. COMPOUND,3=RAP COMPOUND)	2
KIN1(0=INFINITE HELMHOLTZ MIXING RATE, 1=FINITE RATE 2=FINITE RATE,FINITE BOOSTER JET)	2
KIN2(0=INSTANTANEOUS DROPLET COMBUSTION, 1=FINITE RATE)	0
ICP (0 - USE VENT AREA) (1 - COMPUTE VENT AREA FOR CONST. PRES.) (2 - COMPUTE VENT AREA FOR CONST. ACC.)	0
IPAR (0 - NORMAL INPUT) (1 - COMPUTE LIQUID & COMBUSTION VOLUMES) (2 - COMPUTE LIQUID VOLUME FROM C/M)	0
NHTW (0 - WALL TEMP. NOT UPDATED (1 - WALL TEMP. UPDATED)	0
JHTW (0 - NO HEAT LOSS) (1 - HEAT LOSS TO TUBE)	1
NTEM (NO. OF TUBE INITIAL TEMP. PROFILE ENTRIES	0
NENV (NO. OF TUBE INTERVALS FOR PRESS ENVELOPE)	0
NPISR (0 - NO PISTON RESISTANCE (1 - PISTON RESISTANCE FUNCTION OF TRAVEL (2 - PISTON RESISTANCE FUNCTION OF VELOCITY	0
NCD (0 - CD IS CONSTANT) (1 - CD IS FUNCTION OF PISTON TRAVEL)	0
NORVS (0 - NO BACKFLOW TO LP BOOSTER CHAMBER) (1 - BACKFLOW IS ALLOWED)	0
IGNITR (0 - BOOSTER IGNITER NOT MODELED) (1 - BOOSTER IGNITER IS MODELED)	0
IGNLOC (0 - BOOSTER IGNITER NOT ON SIDEWALL) (1 - BOOSTER IGNITER IS ON SIDEWALL)	0
NXPEL (0 - TC EXPULSION CHARGE NOT PRESENT) (1 - TC EXPULSION CHARGE IS PRESENT)	0
NARB (0 - VENT GEOMETRY NOT PRESCRIBED BY ARBV 0) (1 - VENT GEOMETRY SPECIFIED BY ARBVEN)	

LOGOUT PARAMETERS

SAVE ON UNIT 8(0=NO,1=YES)	0
START FROM UNIT 8(0=NO,>0=STEP TO START)	0
PLOTTING ON LOGOUT(0=NO,1=YES)	1
NUMBER OF STEPS BEFORE LOGOUT	9999
TIME INTERVAL BEFORE LOGOUT(MSEC)	0.100
DEBUG PRINT REQUIRED (0=NO,1=YES)	0
INPUT DATA PRINTED (Y=0,N=1)	0

TRAJECTORY DATA PRINTED (Y=0,N=1)	0
EXTRA TRAJECTORY DATA PRINTED (Y=0,N=1)	0
MASS BAL. REG 1>4 DATA PRINTED (Y=0,N=1)	0
MASS BAL. REG 5>8 DATA PRINTED (Y=0,N=1)	0
ENERGY BAL. REG 1>4 DATA PRINTED (Y=0,N=1)	0
ENERGY BAL. REG 1>4 (CONT) DATA PRINTED (Y=0,N=1)	0
ENERGY BAL. REG 5>8 DATA PRINTED (Y=0,N=1)	0
PROFILE AND PLOT DATA PRINTED (Y=0,N=1)	0

TERMINATION PARAMETERS

NUMBER OF INTEGRATION STEPS	99999
TIME INTERVAL(MSEC)	100.000
PROJECTILE TRAVEL(CM)	213.300

INTEGRATION PARAMETERS

NUMBER OF POINTS ASSIGNED TO TRAVELING CHARGE	0
MAXIMUM NUMBER OF POINTS ASSIGNED TO TUBE	41
MINIMUM MESH SPACING IN TRAVELING CHARGE(CM)	0.500
MINIMUM MESH SPACING IN TUBE(CM)	0.100
C-F-L SAFETY FACTOR(-)	2.000
FLUX CONVERGENCE TOLERANCE(GM**2/SEC**2)	0.010
SOURCE TERM STABILITY FACTOR(-)	0.050
MAXIMUM NUMBER OF MESH POINTS ASSIGNED TO EACH CHAMBER	21
MINIMUM MESH SPACING IN RESERVOIR(CM)	0.200

DESCRIPTION OF TUBE

NUMBER OF PAIRS OF OBTURATOR RESISTANCE DATA	3
AIR SHOCK RESISTANCE(0=NO,1=YES)	1
TUBE DIAMETER(CM)	2.500
TUBE ENTRANCE COEFFICIENT(-)	1.000

OBTURATOR RESISTANCE

PROJECTILE TRAVEL(CM)	RESISTANCE(MPA)
0.000	10.000
0.010	5.500
213.300	5.500

PROPERTIES OF GAS IN FRONT OF PROJECTILE

INITIAL PRESSURE(MPA)	0.100
INITIAL TEMPERATURE(DEG.K)	300.000
RATIO OF SPECIFIC HEATS(-)	1.400

MOLECULAR WEIGHT(GM/GMOL)	28.960

PROPERTIES OF PROJECTILE

MASS(GM)	97.300
LOCATION OF BASE WITH RESPECT TO TUBE ENTRANCE(CM)	0.000
TRAVEL REQUIRED TO INITIATE VENTING OF TRAVELING LIQUID CHARGE(CM)	0.000
DENSITY OF AFTERBODY MATERIAL(GM/CC)	0.000
PRESSURE FOR SEPARATION OF TLC FROM BASE OF PROJECTILE(MPA)	0.000

PROPERTIES OF COMPOUND RLPG BOOSTER

INITIAL VOLUME OF FUEL CHAMBER(CC)	95.061
INITIAL VOLUME OF COMBUSTION CHAMBER(CC)	35.400
INJECTION HOLE AREA(CM**2)	4.897
NUMBER OF INJECTION HOLES(-)	1.000
INJECTION HOLE DISCHARGE COEFFICIENT(-)	0.900

PROPERTIES OF FORWARD CYLINDER

MASS OF PISTON(GM)	685.000
INITIAL VOLUME OF DAMPING LIQUID CHAMBER(CC)	0.000
VOLUME OF D.L. RECEIVER CHAMBER(CC)	0.000
FUEL SIDE PISTON AREA(CM**2)	16.504
COMBUSTION CHAMBER SIDE PISTON AREA(CM**2)	18.613
DAMPING CHAMBER SIDE PISTON AREA(CM**2)	0.000
MAXIMUM PISTON DISPLACEMENT(CM)	4.442
% OF MAXIMUM PISTON DISPLACEMENT	0.980

PROPERTIES OF CENTER CYLINDER

MASS OF PISTON(GM)	0.000
INITIAL VOLUME OF DAMPING LIQUID CHAMBER(CC)	0.000
VOLUME OF D.L. RECEIVER CHAMBER(CC)	0.000
FUEL SIDE PISTON AREA(CM**2)	0.000
COMBUSTION CHAMBER SIDE PISTON AREA(CM**2)	0.000
DAMPING CHAMBER SIDE PISTON AREA(CM**2)	0.000
MAXIMUM PISTON DISPLACEMENT(CM)	0.000
% OF MAXIMUM PISTON DISPLACEMENT	0.000

PROPERTIES OF REAR CYLINDER

MASS OF PISTON(GM)	0.000
INITIAL VOLUME OF DAMPING LIQUID CHAMBER(CC)	0.000
VOLUME OF D.L. RECEIVER CHAMBER(CC)	0.000

FUEL SIDE PISTON AREA(CM**2)	0.000
COMBUSTION CHAMBER SIDE PISTON AREA(CM**2)	0.000
DAMPING CHAMBER SIDE PISTON AREA(CM**2)	0.000
MAXIMUM PISTON DISPLACEMENT(CM)	0.000
% OF MAXIMUM PISTON DISPLACEMENT	0.000

GEOMETRIC DATA FOR CONTINUUM ANALYSIS OF CHAMBERS

DIST. FROM TUBE TO FORWARD CYLINDER(CM)	1.387
DIST. FROM TUBE TO CENTER CYLINDER(CM)	1.387
DIST. FROM TUBE TO REAR CYLINDER(CM)	5.829
DIST. FROM TUBE TO REAR OF INT. CHAMBER(CM)	0.000
DIST. FROM TUBE TO BREECH(CM)	0.000
LENGTH OF INJECTION HOLES IN FWD. CYL.(CM)	0.000

DIST. FROM TUBE(CM)	RADIUS OF C.C.(CM)
0.00000	2.8500
30.000	2.8500

DIST. FROM FRONT(CM)	RADIUS OF FWD. CYL.(CM)
0.00000	2.7300
30.000	2.7300

DIST. FROM FRONT(CM)	RADIUS OF CENT. CYL.(CM)
0.00000	0.80000
30.000	0.80000

PROPERTIES OF DAMPING LIQUID

DENSITY AT ONE ATMOSPHERE(GM/CC)	1.460
BULK MODULUS AT ONE ATMOSPHERE(MPA)	5103.500
DERIVATIVE OF MODULUS W.R.T PRESSURE(-)	8.217

COMPOUND BOOSTER CONTROL DATA

NPXSGN (0 - FUEL INJECTION AREA GIVEN AS FUNCTION OF Z-FWD MINUS Z-CENTER) (1 - FUEL INJECTION AREA GIVEN AS FUNCTION OF Z-CENTER MINUS Z-FWD)	0
NO. OF DATA TO DESCRIBE FWD CYL DAMPER VENT AREA	0
NO. OF DATA TO DESCRIBE CENTER CYL DAMPER VENT AREA	0
NO. OF DATA TO DESCRIBE REAR CYL DAMPER VENT AREA	0
NO. OF DATA TO DESCRIBE FWD CYL DAMPER DISCHARGE COEFF	0
NO. OF DATA TO DESCRIBE CENTER CYL DAMPER DISCHARGE COEFF	0
NO. OF DATA TO DESCRIBE REAR CYL DAMPER DISCHARGE COEFF	0
NPISRC(1) (0 - NO RESISTANCE FOR FWD CYL) (1 - RES. DEPENDS ON DISP.)	0

(2 - RES. DEPENDS ON VEL. AND PRES.)	
(3 - COMBINATION OF 1 AND 2)	
NPISRC(2) - RESISTANCE LAW FOR CENTER CYL	0
NPISRC(3) - RESISTANCE LAW FOR REAR CYL	0
NSIDEV (0 - RAP INJECTION AS ABOVE)	0
(>0 - NUMBER OF SIDEWALL VENTING DATA)	

PROPERTIES OF LIQUID FUEL

DENSITY AT ONE ATMOSPHERE(GM/CC)	1.230
BULK MODULUS AT ONE ATMOSPHERE(MPA)	1206.500
DERIVATIVE OF MODULUS W.R.T PRESSURE(-)	2.500
CHEMICAL ENERGY(J/GM)	3240.807
RATIO OF SPECIFIC HEATS OF PRODUCTS(-)	1.267
MOLECULAR WEIGHT OF PRODUCTS(GM/GMOL)	19.062
COVOLUME OF PRODUCTS(CC/GM)	1.257

FINITE RATE HELMHOLTZ MIXING DATA

DROPLET DIAMETER(CM)	0.001
HELMHOLTZ MIXING COEFFICIENT(GM/CM)	0.000

BOOSTER JET PROPERTIES

BREAKUP LENGTH COEFFICIENT(-)	0.200
SURFACE TENSION(GM/SEC**2)	20.000
VISCOSITY(GM/CM-SEC)	0.71000E-01
NOZZLE INVERSE AREA INTEGRAL(1/CM)	0.000
COEFFICIENT OF RESTITUTION FOR JET IMPACT(-)	1.000
TUBE ADMITTANCE(-)	1.000
INCREMENTLENGTH/MESH SPACING(-)	1.000

INITIAL DATA

PRESSURE OF GAS(MPA)	3.400
PRESSURE OF LIQUID BOOSTER CHARGE(MPA)	2.000
PRESSURE OF LIQUID TRAVELING CHARGE(MPA)	0.000
TEMPERATURE(DEG.K)	1986.000
PRESSURE OF DAMPING LIQUID(MPA)	0.000

DESCRIPTION OF INITIAL CAVITY

NUMBER OF PAIRS OF DATA TO DESCRIBE CAVITY	0
CAVITY MECHANICALLY STABILIZED(0=NO,1=YES)	1

CROSS-SECTIONAL AREA COMBUSTION CHAMBER(CM**2)	25.5200
PISTON TRAVEL - INJECTION AREA TABLE	

F. PISTON TRAVEL	PISTON TRAVEL(CM)	VENT AREA (CM**2)
0.0000	0.000	0.100000E-01
0.1000	0.449	4.89676
1.0000	4.488	4.89676

THERMAL PROPERTIES OF TUBE

INITIAL TUBE TEMPERATURE (DEG.K)	300.000
THERMAL CONDUCTIVITY (J/CM-SEC-DEG.K)	0.622100
THERMAL DIFFUSIVITY (CM**2/SEC)	0.147100
EMISIVITY FACTOR (-)	1.00000
HEAT LOSS MULTIPLIER FACTOR (-)	1.00000

TOTAL PROPELLANT WEIGHT (GM)	117.2489
TOTAL CHEMICAL ENERGY (KJ)	379.9811
BOOSTER WEIGHT (GM)	117.1216
TRAVELING CHARGE WEIGHT (GM)	0.0000000
IGNITER WEIGHT (GM)	0.1382631
LOADING DENSITY (GM/CC)	0.8987280
C/M	1.205025

No of Copies	Organization
1	Office of the Secretary of Defense OUSD(A) Director, Live Fire Testing ATTN: James F. O'Bryon Washington, DC 20301-3110
(Unclass., unlimited) 12 (Unclass., limited) 2 (Classified) 2	Administrator Defense Technical Info Center ATTN: DTIC-DDA Cameron Station Alexandria, VA 22304-6145
1	HQDA (SARD-TR) WASH DC 20310-0001
1	Commander US Army Materiel Command ATTN: AMCDRA-ST 5001 Eisenhower Avenue Alexandria, VA 22333-0001
1	Commander US Army Laboratory Command ATTN: AMSLC-DL Adelphi, MD 20783-1145
2	Commander Armament RD&E Center US Army AMCCOM ATTN: SMCAR-MSI Picatinny Arsenal, NJ 07806-5000
2	Commander Armament RD&E Center US Army AMCCOM ATTN: SMCAR-TDC Picatinny Arsenal, NJ 07806-5000
1	Director Benet Weapons Laboratory Armament RD&E Center US Army AMCCOM ATTN: SMCAR-CCB-TL Watervliet, NY 12189-4050
1	Commander US Army Armament, Munitions and Chemical Command ATTN: SMCAR-ESP-L Rock Island, IL 61299-5000
1	Commander US Army Aviation Systems Command ATTN: AMSAV-DACL 4300 Goodfellow Blvd. St. Louis, MO 63120-1798

No of Copies	Organization
1	Director US Army Aviation Research and Technology Activity Ames Research Center Moffett Field, CA 94035-1099
1	Commander US Army Missile Command ATTN: AMSMI-RD-CS-R (DOC) Redstone Arsenal, AL 35898-5010
1	Commander US Army Tank-Automotive Command ATTN: AMSTA-TSL (Technical Library) Warren, MI 48397-5000
1	Director US Army TRADOC Analysis Command ATTN: ATAA-SL White Sands Missile Range, NM 88002-5502
(Class. only) 1	Commandant US Army Infantry School ATTN: ATSH-CD (Security Mgr.) Fort Benning, GA 31905-5660
(Unclass. only) 1	Commandant US Army Infantry School ATTN: ATSH-CD-CSO-OR Fort Benning, GA 31905-5660
1	Air Force Armament Laboratory ATTN: AFATL/DLODL Eglin AFB, FL 32542-5000
	Aberdeen Proving Ground
2	Dir, USAMSAA ATTN: AMXSY-D AMXSY-MP, H. Cohen
1	Cdr, USATECOM ATTN: AMSTE-TD
3	Cdr, CRDEC, AMCCOM ATTN: SMCCR-RSP-A SMCCR-MU SMCCR-MSI
1	Dir, VLAMO ATTN: AMSLC-VL-D

No. of Copies	Organization
2	Director Defense Advanced Research Projects Agency ATTN: J. Lupo J. Richardson 1400 Wilson Boulevard Arlington, VA 22209
4	HQDA ATTN: SARD-ZT, G. Singley SARD-TT, I. Szkrybalo SARD-TC, C. Church B. Zimmerman WASH DC 20310
1	HQ, US Army Materiel Command ATTN: AMCICP-AD, B. Dunetz 5001 Eisenhower Avenue Alexandria, VA 22333-0001
13	Commander Armament Research and Development Center US Army AMCCOM ATTN: SMCAR-TSS SMCAR-AEE-BR, B. Brodman W. Seals A. Beardell SMCAR-AEE-B, D. Downs SMCAR-AEE-W, N. Slagg SMCAR-AEE, A. Bracuti J. Lannon M. Gupta J. Salo D. Chicu SMCAR-FSS-D, L. Frauen SMCAR-FSA-S, H. Liberman Picatinny Arsenal, NJ 07806-5000
3	Commander Armament Research and Development Center US Army AMCCOM ATTN: SMCAR-FSS-DA, Bldg 94 J. Feneck R. Kopman J. Irizarry Picatinny Arsenal, NJ 07806-5000

No. of Copies	Organization
4	Director Benet Weapons Laboratory Armament Research and Development Center US Army AMCCOM ATTN: SMCAR-CCB, L. Johnson SMCAR-CCB-S, F. Heiser SMCAR-CCB-DS, E. Conroy A. Graham Watervliet, NY 12189-4050
1	Commander Materials Technology Laboratory US Army Laboratory Command ATTN: SLCMT-MCM-SB, M. Levy Watertown, MA 02172-0001
1	Commander, USACECOM R&D Technical Library ATTN: ASQNC-ELC-I-T, Myer Center Fort Monmouth, NJ 07703-5301
1	Commander US Army Harry Diamond Laboratories ATTN: SLCHD-TA-L 2800 Powder Mill Road Adelphi, MD 20783-1145
1	Commander US Army Belvoir Research and Development Center ATTN: STRBE-WC Technical Library (Vault) B-315 Fort Belvoir, VA 22060-5606
1	Commander US Army Research Office ATTN: Technical Library P.O. Box 12211 Research Triangle Park, NC 27709-2211
1	Commander Armament Research and Development Center US Army Armament, Munitions and Chemical Command ATTN: SMCAR-CCS-C, T. Hung Picatinny Arsenal, NJ 07806-5000

No. of Copies	Organization
2	Commandant US Army Field Artillery School ATTN: ATSF-CMW ATSF-TSM-CN, J. Spicer Fort Sill, OK 73503
1	Commandant US Army Armor Center ATTN: ATSB-CD-MLD Fort Knox, KY 40121
1	Commander Naval Surface Warfare Center ATTN: D.A. Wilson, Code G31 Dahlgren, VA 22448-5000
1	Commander Naval Surface Warfare Center ATTN: Code G33, J. East Dahlgren, VA 22448-5000
2	Commander US Naval Surface Warfare Center ATTN: O. Dengel K. Thorsted Silver Spring, MD 20902-5000
1	Commander (Code 3247) Naval Weapons Center Guns Systems Branch China Lake, CA 93555-6000
1	AFOSR/NA (L. Caveny) Building 410 Bolling AFB Washington, DC 20332
1	Commandant USAFAS ATTN: ATSF-TSM-CN Fort Sill, OK 73503-5600
1	Director Jet Propulsion Laboratory ATTN: Technical Library 4800 Oak Grove Drive Pasadena, CA 91109

No. of Copies	Organization
2	Director National Aeronautics and Space Administration ATTN: MS-603, Technical Library MS-86, Dr. Povinelli 21000 Brookpark Road Lewis Research Center Cleveland, OH 44135
1	Director National Aeronautics and Space Administration Manned Spacecraft Center Houston, TX 77058
10	Central Intelligence Agency Office of Central Reference Dissemination Branch Room GE-47 HQS Washington, DC 20502
1	Central Intelligence Agency ATTN: Joseph E. Backofen HQ Room 5F22 Washington, DC 20505
1	Calspan Corporation ATTN: Technical Library P.O. Box 400 Buffalo, NY 14225
8	General Electric Ordnance System Division ATTN: J. Mandzy, OP43-220 R.E. Mayer H. West W. Pasko R. Pate I. Magoon J. Scudiere Minh Luu 100 Plastics Avenue Pittsfield, MA 01201-3698
1	General Electric Company Armament Systems Department ATTN: D. Maher Burlington, VT 05401
1	Honeywell, Inc. ATTN: R.E. Tompkins MN38-3300 10400 Yellow Circle Drive Minnetonka, MN 55343

No. of Copies	Organization
1	IITRI ATTN: Library 10 W. 35th Street Chicago, IL 60616
1	Olin Chemicals Research ATTN: David Gavin P.O. Box 586 Chesire, CT 06410-0586
2	Olin Corporation ATTN: Victor A. Corso Dr. Ronald L. Dotson 24 Science Park New Haven, CT 06511
1	Paul Gough Associates ATTN: Paul Gough 1048 South Street Portsmouth, NH 03801-5423
1	Safety Consulting Engineer ATTN: Mr. C. James Dahn 5420 Pearl Street Rosemont, IL 60018
1	Sandia National Laboratories ATTN: R. Rychnovsky, Division 8152 P.O. Box 969 Livermore, CA 94551-0969
1	Sandia National Laboratories ATTN: S. Griffiths, Division 8244 P.O. Box 969 Livermore, CA 94551-0969
1	Sandia National Laboratories ATTN: R. Carling, Division 8357 P.O. Box 969 Livermore, CA 94551-0969
1	Science Applications, Inc. ATTN: R. Edelman 23146 Cumorah Crest Woodland Hills, CA 91364
2	Science Applications International Corporation ATTN: Dr. F.T. Phillips Dr. Fred Su 10210 Campus Point Drive San Diego, CA 92121
1	Science Applications International Corporation ATTN: Norman Banks 4900 Waters Edge Drive Suite 255 Raleigh, NC 27606
1	Sundstrand Aviation Operations ATTN: Mr. Owen Briles P.O. Box 7202 Rockford, IL 61125
1	Veritay Technology, Inc. ATTN: E.B. Fisher 4845 Millersport Highway P.O. Box 305 East Amherst, NY 14051-0305
1	Director Applied Physics Laboratory The Johns Hopkins University Johns Hopkins Road Laurel, MD 20707
2	Director CPIA The Johns Hopkins University ATTN: T. Christian Technical Library Johns Hopkins Road Laurel, MD 20707
1	University of Illinois at Chicago ATTN: Professor Sohail Murad Department of Chemical Engineering Box 4348 Chicago, IL 60680
1	University of Maryland at College Park ATTN: Professor Franz Kasler Department of Chemistry College Park, MD 20742
1	University of Missouri at Columbia ATTN: Professor R. Thompson Department of Chemistry Columbia, MO 65211
1	University of Michigan ATTN: Professor Gerard M. Faeth Department of Aerospace Engineering Ann Arbor, MI 48109-3796

No. of Copies	Organization
1	University of Missouri at Columbia ATTN: Professor F.K. Ross Research Reactor Columbia, MO 65211
1	University of Missouri at Kansas City Department of Physics ATTN: Professor R.D. Murphy 1110 East 48th Street Kansas City, MO 64110-2499
1	Pennsylvania State University Department of Mechanical Engineering ATTN: Professor K. Kuo University Park, PA 16802
2	Princeton Combustion Research Laboratories, Inc. ATTN: N.A. Messina M. Summerfield 4275 U.S. Highway One North Monmouth Junction, NJ 08852
1	University of Arkansas Department of Chemical Engineering ATTN: J. Havens 227 Engineering Building Fayetteville, AR 72701
3	University of Delaware Department of Chemistry ATTN: Mr. James Cronin Professor Thomas Brill Mr. Peter Spohn Newark, DE 19711
1	University of Texas at Austin Bureau of Engineering Research ATTN: BRC EME133, Room 1.100 H. Fair 10100 Burnet Road Austin, TX 78758

No. of Copies	Organization
1	Clive Woodley GS2 Division Building R31 RARDE Fort Halstead Sevenoaks, Kent TN14 7BT England

USER EVALUATION SHEET/CHANGE OF ADDRESS

This Laboratory undertakes a continuing effort to improve the quality of the reports it publishes. Your comments/answers to the items/questions below will aid us in our efforts.

1. BRL Report Number BRL-TR-3077 Date of Report APRIL 1990

2. Date Report Received _____

3. Does this report satisfy a need? (Comment on purpose, related project, or other area of interest for which the report will be used.) _____

4. Specifically, how is the report being used? (Information source, design data, procedure, source of ideas, etc.) _____

5. Has the information in this report led to any quantitative savings as far as man-hours or dollars saved, operating costs avoided, or efficiencies achieved, etc? If so, please elaborate. _____

6. General Comments. What do you think should be changed to improve future reports? (Indicate changes to organization, technical content, format, etc.) _____

CURRENT ADDRESS

Name

Organization

Address

City, State, Zip Code

If indicating a Change of Address or Address Correction, please provide the New or Correct Address in Block 6 above and the Old or Incorrect address below.

OLD ADDRESS

Name

Organization

Address

City, State, Zip Code

(Remove this sheet, fold as indicated, staple or tape closed, and mail.)

FOLD HERE

DEPARTMENT OF THE ARMY
Director
U.S. Army Ballistic Research Laboratory
ATTN: SLCBR-DD-T
Aberdeen Proving Ground, MD 210[illegible]-5066
OFFICIAL BUSINESS

NO POSTAGE
NECESSARY
IF MAILED
IN THE
UNITED STATES

BUSINESS REPLY MAIL
FIRST CLASS PERMIT No 0001, APG, MD

POSTAGE WILL BE PAID BY ADDRESSEE

Director
U.S. Army Ballistic Research Laboratory
ATTN: SLCBR-DD-T
Aberdeen Proving Ground, MD 21005-9989

FOLD HERE